Master of Science

The Pd/SiO_2 catalysts for hydrogenation of D-glucose

The Graduate School of University of Ulsan

School of Chemical Engineering

Ji Soo Kwon

The Pd/SiO_2 catalysts for hydrogenation of D-glucose

Supervisor: Professor Hak Sung Lee

A Dissertation

Submitted to
the Graduate School of the University of Ulsan
In partial Fulfillment of the Requirements
for the Degree of

Master

by

Kwon, Ji Soo

School of Chemical Engineering
University of Ulsan, Korea
February 2018

The Pd/SiO_2 catalysts for hydrogenation of D-glucose

This certifies that master's thesis

of Ji Soo Kwon is approval.

Committee Chair Prof. Eun Woo Shin

Committee Member Prof. Man Sig Lee

Committee Member Prof. Hak Sung Lee

School of Chemical Engineering

University of Ulsan, Korea

February 2018

Acknowledgement

추웠던 2016년 겨울, 처음 실험실에 발을 들였던 때가 엊그제 같은데 많은 분들이 도와주신 덕분에 벌써 2년의 시간이 지나 작은 결실을 맺고 새로운 시작을 준비하고 있습니다. 부족한 저에게 많은 도움을 주신 고마운 분들께 감사의 마음을 전하고 싶습니다.

먼저 대학 졸업을 앞두고 진로에 대하여 고민하고 있을 때 대학원 진학의 길을 열어주신 이학성 교수님께 감사 드립니다. 학부시절부터 지금까지 아낌없는 지도와 관심을 보여주신 덕분에 석사 과정을 잘 마무리 할 수 있었습니다.

그리고 여러 면에서 부족한 점이 많은 저를 흔들리지 않도록 곁에서 아낌없이 격려해 주시고 인도해 주신 이만식 박사님께 진심으로 감사합니다. 오랜 타지 생활에 지친 제게 아버지와 같은 마음으로 대해주셔서 많은 의지가 되었습니다. 앞으로도 박사님의 가르침을 마음 깊이 새겨 어디서든 자랑스러운 제자가 되도록 노력하겠습니다.

또한 바쁘신 와중에 소중한 시간을 내주셔서 논문 심사와 고견을 내어주신 신은우 교수님께 감사 인사를 드립니다. 교수님의 지도 덕분에 석사학위 논문을 무사히 마무리 할 수 있었습니다.

이 외에도 한국생산기술연구원에서의 석사 과정 동안 많은 도움을 주신 김억수 본부장님, 문우균 위원님, 변용위 위원님께 지면으로나마 감사의 인사를 전하고 싶습니다.

특히나 학위 기간 동안 가장 오랜 시간을 함께 보낸 친환경에너지재료실험실 식구들에게 고마움을 전합니다. 실험실의 든든한 버팀목이 되어주신 백재호 박사님, 류영복 박사님, 팀원들의 단합을 책임져주신 김경호 연구원님, 언제나 긍정적인 에너지가 넘치시는 박동국 박사님, 항상 팀원들을 위해 배려해주신 민아 언니께 감사의 마음을 전합니다. 여러분들 덕분에 부족했던 제가 한 단계 성장할 수 있었습니다. 또한 저의 영원한 사수, 지선이 언니께 감사드립니다. 아무것도 몰랐던 제게 친 언니처럼 신경 써주시고 이끌어 주

신 덕분에 실험실 생활에 잘 적응할 수 있었습니다. 그리고 늘 의지했던 미연이에게도 고마움을 전합니다. 2년동안 함께 지내면서 항상 모자란 나를 챙겨주느라 많이 고생했고 앞으로 박사 학위도 지금처럼만 하면 수월히 마칠 것이라 믿어 의심치 않습니다. 또한 항상 제 장난을 받아줬던 착한 부윤이 오빠와 내년부터 학위를 시작하게 된 예은이 은영이 현곤이에게 응원을 보냅니다. 덧붙여서 제 멘탈이 무너지지 않게 많은 도움을 줬던 왜구대 친구들과 힘들 때마다 만나서 기운을 북돋아 줬던 44대 집행부원들, 그리고 유일한 대학원 동기 슬이에게 감사의 말을 전하고 싶습니다.

마지막으로 언제나 저를 믿고 아낌없이 지원해주시는 아버지, 엄마 그리고 제일 친한 친구이자 동생인 지원이에게 고맙고 사랑한다는 말을 전합니다. 앞으로 자랑스러운 큰 딸이자 든든한 언니가 될 수 있도록 노력하겠습니다.

아직 부족한 것이 많기 때문인지 지난 2년의 학위 과정을 돌이켜보면 아쉽게 느껴집니다. 지금까지 배운 것들을 마음에 새겨 다시 새로운 출발을 위해 더욱 노력하여 발전하는 모습을 보여드리겠습니다.

2017. 12

권지수

Abstract in Korea

본 연구에서는 고분산성을 가지는 팔라듐 촉매를 제조하고, D-glucose의 수소화 반응에 대한 촉매의 활성을 비교하였다.

대표적인 귀금속 촉매인 팔라듐은 가격이 높고 자원이 한정적이기 때문에 대부분 지지체에 분산된 채로 사용된다. 이때 팔라듐의 분산 정도와 입자의 크기가 촉매 활성에 큰 영향을 미치기 때문에 지지체의 물리·화학적 특성 변화를 통하여 고 분산성을 가지는 팔라듐 촉매를 제조하였고, 팔라듐 분산도가 D-glucose의 수소화 반응에 미치는 영향을 확인하였다.

1) 균일한 기공구조를 가지는 Ordered mesoporous silica (OMS)를 제조하고 팔라듐 촉매의 지지체로 사용하여 담지체의 구조가 촉매의 금속 분산도에 미치는 영향을 살펴보았다. 일반적으로 높은 비표면적을 가지는 물질은 촉매의 지지체로 적합하다. 하지만 OMS를 이용한 촉매는 500m^2/g 이상의 높은 비표면적을 가짐에도 불구하고 6% 이하의 비교적 낮은 팔라듐 분산도를 가진다. 그 이유로 실리카는 낮은 metal-support interaction을 가지고 있고 특히 균일한 기공 구조를 가지고 있는 OMSs의 높은 표면 안정성 때문에 팔라듐이 실리카에 균일하게 분산 되지 못하고 서로 뭉쳐서 담지되는 현상을 확인하였다.

2) SiO_2의 작용기 중 하나인 silanol group (-OH) 은 촉매 제조 중 팔라듐 이온과 강하게 결합하여 –PdO를 형성하기 때문에 팔라듐의 환원을 방해한다. 본 연구에서는 SiO_2의 열처리와 암모니아 처리를 통하여 silanol group을 제거하고, 전처리 된 SiO_2를 이용하여 촉매를 제조해 특성을 비교하였다. 실험 결과 700 이상의 열처리와 200 이상에서의 암모니아 처리에 의하여 SiO_2 표면의 silanol group이 완전히 제거되는 것을 확인하였다. silanol group이 제거된 촉매인 Pd/SiO_2_700과 Pd/SiO_2_A200은 표면 개질을 하지 않은 촉매의 분산도보다 약 3-4배에 달하는 13.02%와 8.82%의 높은 팔라듐 분산도를 가졌다. 따라서 silanol group의 제거가 팔라듐의 분산도의 증가에 긍정적인 영향을 미치는 것을 확인하였다.

3) D-glucose의 수소화 반응을 통하여 제조된 촉매의 활성평가를 진행하였다. 앞서 제조한 팔라듐 촉매를 사용하여 D-glucose의 수소화 반응을 진행하였고 그 결과를 통해 팔라듐

분산도가 촉매 활성에 미치는 영향을 확인하였다. 실험결과 가장 높은 분산도 (13.02%)를 가지는 Pd/SiO_2_700를 이용한 수소화 반응이, 낮은 팔라듐 분산도 (2.90%) 를 가지는 Pd/SiO_2_100와 비교해 65.10%의 높은 솔비톨 수율을 얻을 수 있었다. 이러한 결과를 통하여 팔라듐이 고르게 분산될수록 반응물과 촉매 활성점의 유효 충돌 횟수가 증가하기 때문에 고 분산성 촉매를 사용할수록 촉매 활성이 증가함을 확인하였다.

Abstract in English

In this study, the effect of physical and chemical treatment on catalyst preparation was investigated, and also the activity of prepared catalysts was evaluated by hydrogenation of D-glucose.

As a representative noble metal catalyst, palladium required to be distributed on a supports because it has high cost, finite resources, and sintering at high temperature. Since the dispersion and the particle size of palladium affect the catalytic activity, palladium catalysts with high metal dispersion were prepared through physical and chemical modification of the support properties. And the effect of palladium dispersion on hydrogenation of D-glucose was confirmed

1) Ordered mesoporous silica (OMS) with uniform pore structure was prepared and the effect of the pore structure on the palladium dispersion was investigated. In general, a material having a high specific surface area is suitable for support of catalyst. However, the catalysts using OMSs have relatively low palladium dispersion of less than 6% although it has a high specific surface area of 500 m^2 / g or more. It is reason that silica has a low metal-support interaction and especially, OMSs with uniform pore structure have higher surface stability. So that palladium particles cannot be uniformly distributed on silica, and be supported on OMSs with severely aggregated to each other

2) The silanol group (-OH), which is one of the functional groups of SiO_2, interferes with the reduction of palladium because it strongly bonds with palladium ions (–PdO) during the preparation of the catalyst. In this study, the silanol group was removed through the thermal and the ammonia treatment of SiO_2, and the catalysts were prepared with pretreated SiO_2. As a result, it was confirmed that the silanol group on the SiO_2 surface was completely removed by calcination above 700 ° C and ammonia

treatment above 200 ° C. The Pd / SiO2_700 and Pd / SiO2_A200 catalysts which the silanol groups were removed had a high palladium dispersion of 13.02% and 8.82%, respectively, which were about 3-4 times higher than those of the catalysts without surface modification. Therefore, it was confirmed that the removal of the silanol group positively affects the increase of the dispersion of palladium.

3) The catalytic activity test was conducted by hydrogenation of D-glucose. Hydrogenation was carried out using the prepared catalysts with different metal dispersion, and the effect of palladium dispersion on catalytic activity was confirmed. Experimental results show that the hydrogenation with Pd/SiO_2_700 with the highest dispersion (13.02%) had much higher sorbitol yield of 65.10% compared to Pd / SiO_2_N with low palladium dispersion (2.81%). It was confirmed that as the palladium particles are evenly distributed, the number of effective collisions between the reactant and the catalytic active sites increases, so that the catalyst activity increases with the use of the highly dispersed catalyst.

Contents

Figure list

Table list

1. Introduction

1.1. Noble metal catalyst

Various types of catalyst are employed widely in industry for processes such as hydrogenation, dehydrogenation, and petroleum cracking. More specifically, metal oxides and noble metal catalysts (i.e., containing Pd, Pt, Rh, Ag, and Au, among others) are commonly used because of their favorable reaction rates and reaction selectivity. However noble metals are expensive and finite resources, and tend to exhibit sintering at high temperatures, so many catalysts are prepared by adding small amount of the catalytically active component to a fairly large amount of a more or less inert solid called the support [1]. There are idealized properties of supports, some of which are listed below [2]:

- The support with its large surface area allows the active component to spread thus exposing a large proportion of the latter to the reactants. This minimizes the amount of the active component needed and is particularly important when the active component is expensive
- The support holds on its surface the micro-crystalline particles of the active component and prevents its sintering.
- The support surface may interact with the active component to form surface complexes that have better catalytic activity and selectivity than either that of the support or the active component.
- The porous nature of the support may control the transport of the reactant and the product molecules affecting the overall conversion Support materials should have no catalytic activity leading to undesirable side reactions.

- All kinds of materials that are thermally stable and chemically relatively inert can be used as supports for heterogeneous catalysts used in industry consist of relatively small particles stabilized in some way against sintering.

In this work, Palladium catalyst was prepared with the silica which has these idealized properties, and investigated catalyst activity. The study of metal particles on oxide supports is of importance in heterogeneous catalysis because the size and nature of the interaction of a metal particle with an oxide support are critical in determining catalytic activity and selectivity [3]. The catalytic activity increase when the size of the metal is small and uniformly dispersed, because active site of catalyst reacting with the reactant is widened. The particle size and dispersion of metal can be controlled by method of catalyst preparation, kind of the precursor, support, and support pretreatment. we investigated the effect of support structure and support pretreatment on catalyst preparation.

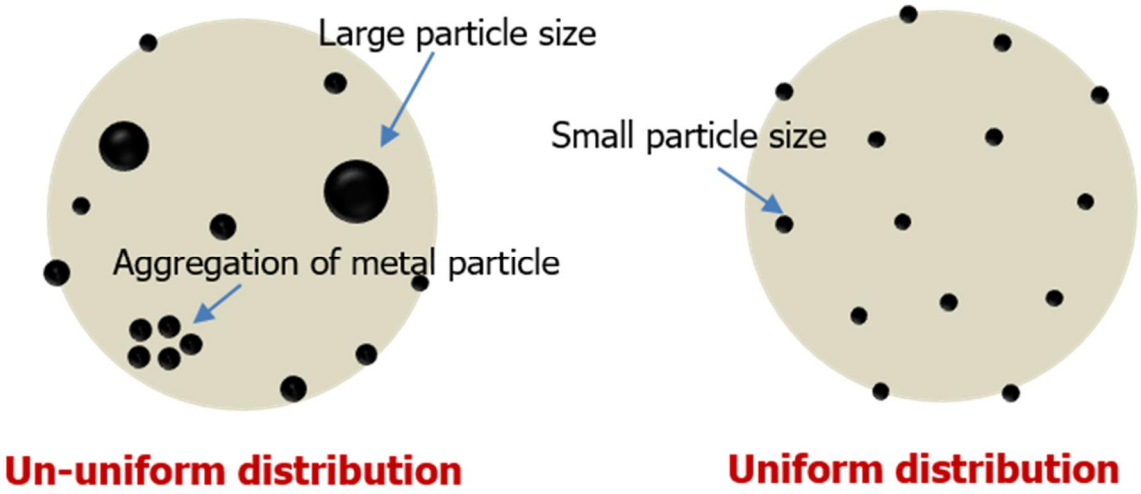

Fig. 1. 1. Metal dispersion of noble metal.

1.2. Property of silica as support

1.2.1. Physical properties of silica

Silica is one of representative porous materials. There are various type of ordered mesoporous silicas (OMSs). The OMS can use different organic templates to control the size and morphology of the pore. Typical OMS include M14S and SBA-15, etc. Mesoporous silica was first discovered in 1990 by researchers in Japan and later was produced in Mobil Corporation Laboratories and named as M41S. MCM-41, MCM-48 and MCM-50 are among the widely known mesoporous silica in M41S family which have different methods of synthesis and applications based on instability and limitation of mesoporous structure. In 1998, a prominent research which produces hexagonal array of pores namely as Santa Barbara Amorphous no 15 (SBA-15) with larger pore size from 4.6-30 nm was a research gambit in mesoporous material development [4]. Because OMSs have high surface area, pore volume, ordered structure and high capacity to functionalize its surface suitable, OMSs are considered as suitable support [5]. In general, the increase of the specific surface area has a positive effect on metal dispersion of the catalyst. But also the pore structure of the support is important because the distribution and adsorption rate of the metal are determined by these factors. Depending on the predominant pore sizes, the porous solid materials are classified by IUPAC [4, 5] :

1) Microporous materials, having pore diameters up to 2.0 nm
2) Mesoporous materials, having pore sizes intermediate between 2.0 and 50.0 nm
3) Macroporous materials, having pore sizes exceeding 50.0 nm

Porous materials are most frequently characterized in terms of pore sizes derived from

gas sorption data, and IUPAC conventions have been proposed for classifying pore sizes and gas sorption isotherms that reflect the relationship between porosity and sorption (Fig. 1. 3.). The IUPAC classification of type of physisorption isotherms is illustrated in Fig. 1. 4. The six types of isotherm are characteristic of adsorbents that are microporous (type I), nonporous or macroporous (types II, III, and VI), or mesoporous (types IV and V) An empirical classification of hysteresis loops was given by IUPAC, which is based on an earlier classification of hysteresis by de Boer [4, 5]. Fig. 1. 5. shows Types of hysteresis loops according to IUPAC, type H1 is often associated with porous materials consisting of well-defined cylindrical-like pore channels or agglomerates of approximately uniform spheres. Type H_2 ascribes materials that are often disordered where the distribution of pore size and shape is not well defined and also indicative of bottleneck constrictions. Materials that give rise to H_3 hysteresis have slit-shaped pores (the isotherms revealing type H_3 do not show any limiting adsorption at high P/P_o, which is observed with non-rigid aggregates of plate-like particles). The desorption curve of H_3 hysteresis contains a slope associated with a force on the hysteresis loop, due to the so-called tensile strength effect (this phenomenon occurs perhaps for nitrogen at 77 K in the relative pressure range from 0.4 to 0.45). On the other hand, type H_4 hysteresis is also often associated with narrow slit pores [4, 5, 6]. In this study, we investigated the effect of the pore structure on the preparation of catalyst using three OMS, SBA-15, MCM-48 and HMS.

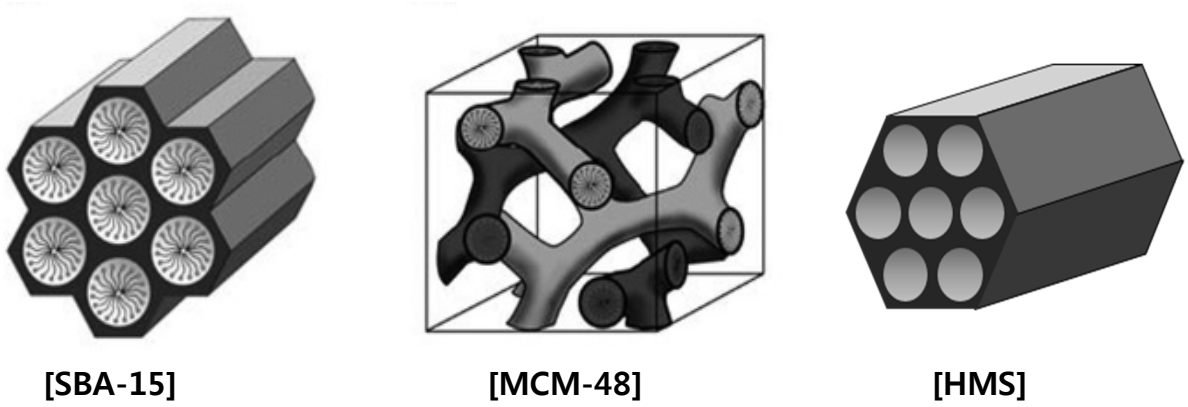

Fig. 1. 2. Various ordered mesoporous silicas (OMSs) [4].

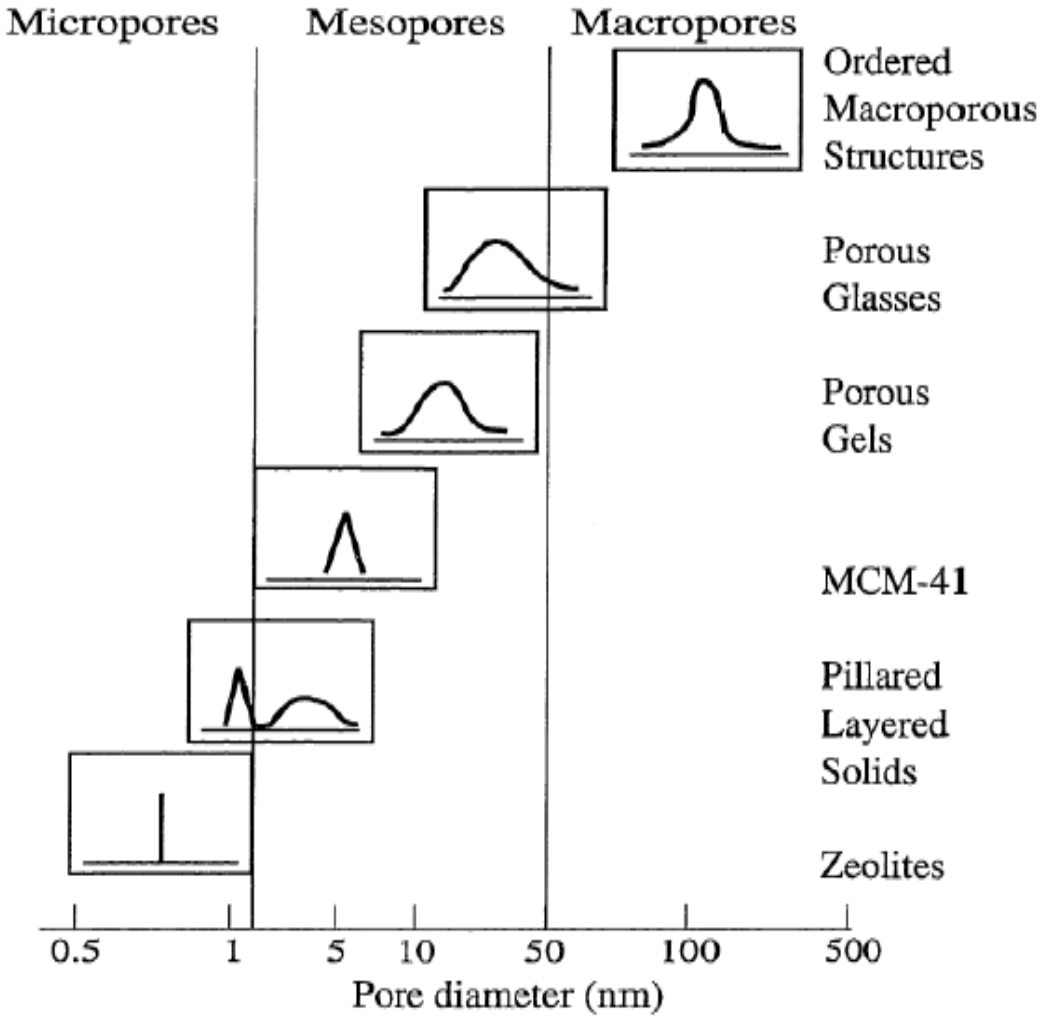

Fig. 1. 3. Schematic illustrating pore size distribution of some porous materials [6].

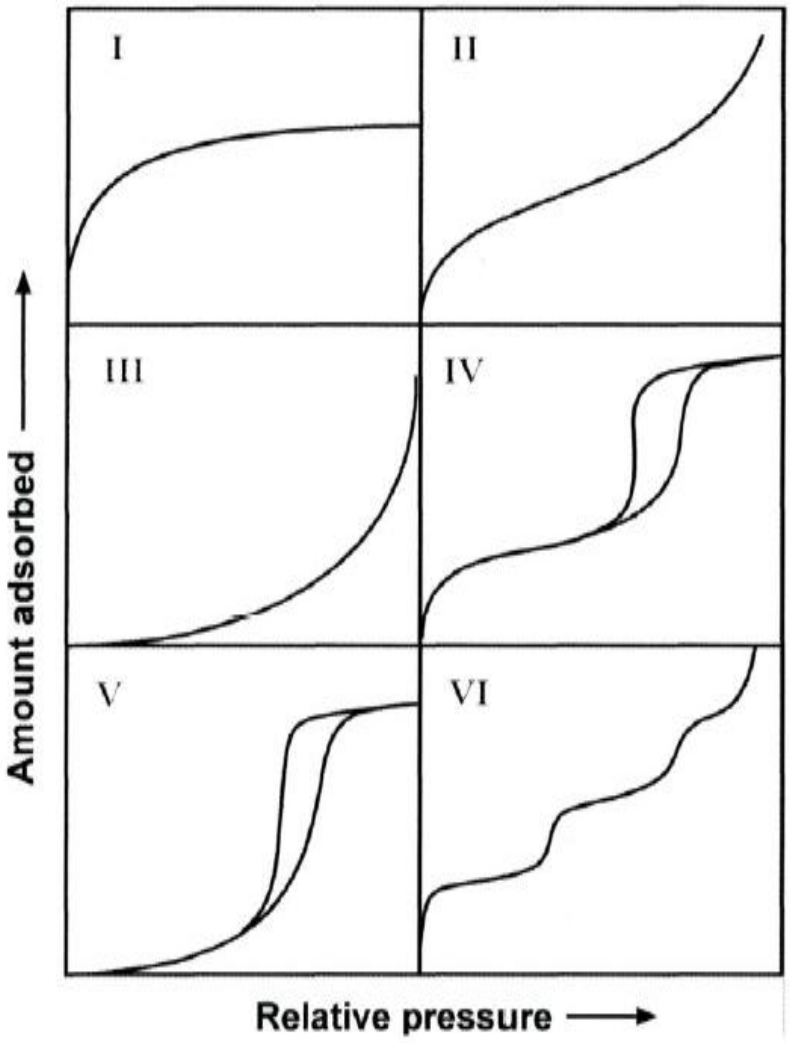

Fig. 1. 4. The IUPAC classification of adsorption isotherms [8].

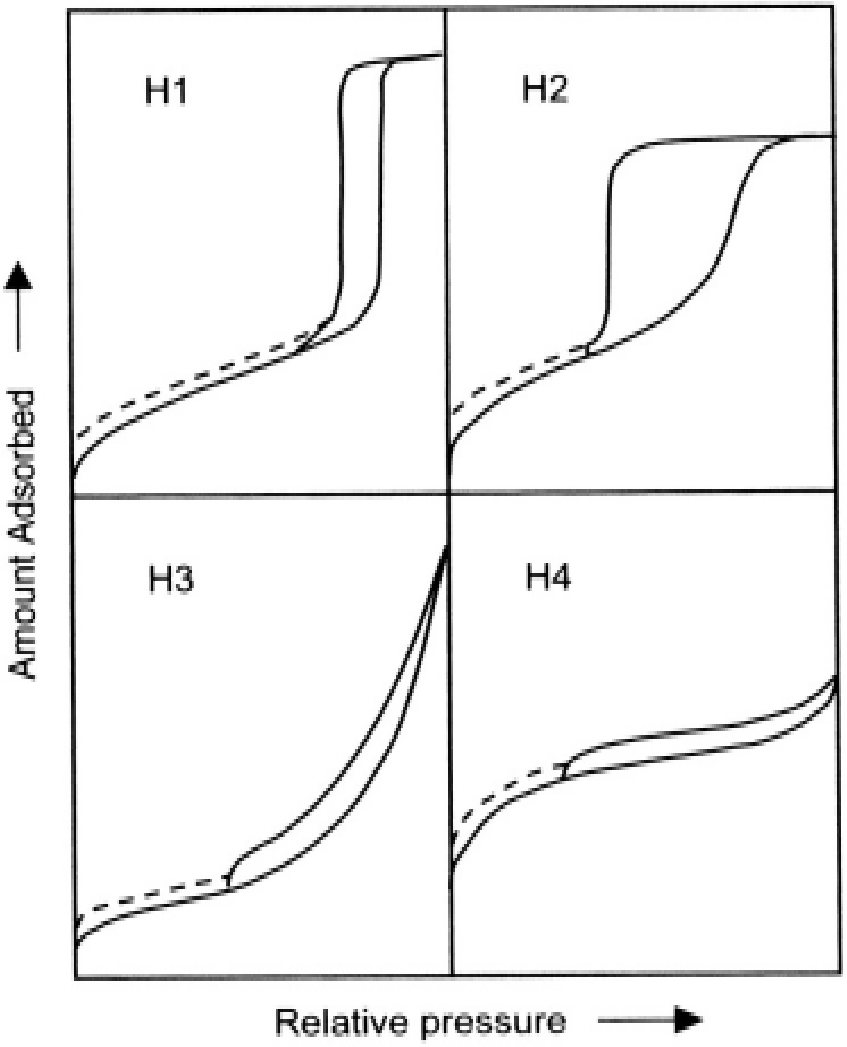

Fig. 1. 5. The relationship between the pore shape and the adsorption-desorption isotherm [8].

1.2.2. Chemical properties of silica

Silica is one of the most extensively used catalyst supports due to its high specific surface area, ample porosity, good stability, and morphological stability at high temperatures. Also silica is an inert support and does not take part in the catalytic reaction [9].

The interaction of a metal particle with oxide support is significant for determining catalytic activity and selectivity. However, silica is an irreducible oxide, and exhibits weak metal-support interactions compared to other metal oxides such as alumina and titania [3]. These properties render the deposition of noble metals on the support surface particularly challenging, and so modification if the silica surface is required to increase the catalyst preparation efficiency.

There are various types of Silanol groups which is a functional group of silica. Surface OH groups are subdivided as following [10] :

1) isolated free (single silanols), SiOH
2) geminal free (geminal silanols or silanediols), -$Si(OH)_2$
3) vicinal, or bridged, or OH groups bound through the hydrogen bond (H-bonded single silanols, H-bonded geminals, and their H bonded combinations).

This silanol groups present on the surface can suppress reduction of the noble metal precursor, thereby decreasing metal dispersion, which is an important factor in determining catalyst activity [4, 5, 6]. As the silanol groups can contribute to strong interactions between the metal species and oxygen on the SiO_2 support, metal reducibility on the surface can be reduced through such interactions [12].

Therefore, support pretreatment is necessary to decrease the surface silanol groups.

To date, a number of support pretreatment methods have been reported, including calcination [9] and pretreatment with nC1–C5 [13], organic solvents [12], and ammonia [14]. Such pretreatment controls the chemical properties of the silica surface, including the functional groups present on the support. Thus, we herein report the modification of SiO_2 by calcination and ammonia water treatment to examine the effect of the surface silanol concentration on the SiO_2 support on the preparation and properties of SiO_2-supported Pd catalysts. The effect of these pretreatments on Pd dispersion and reducibility will also be examined.

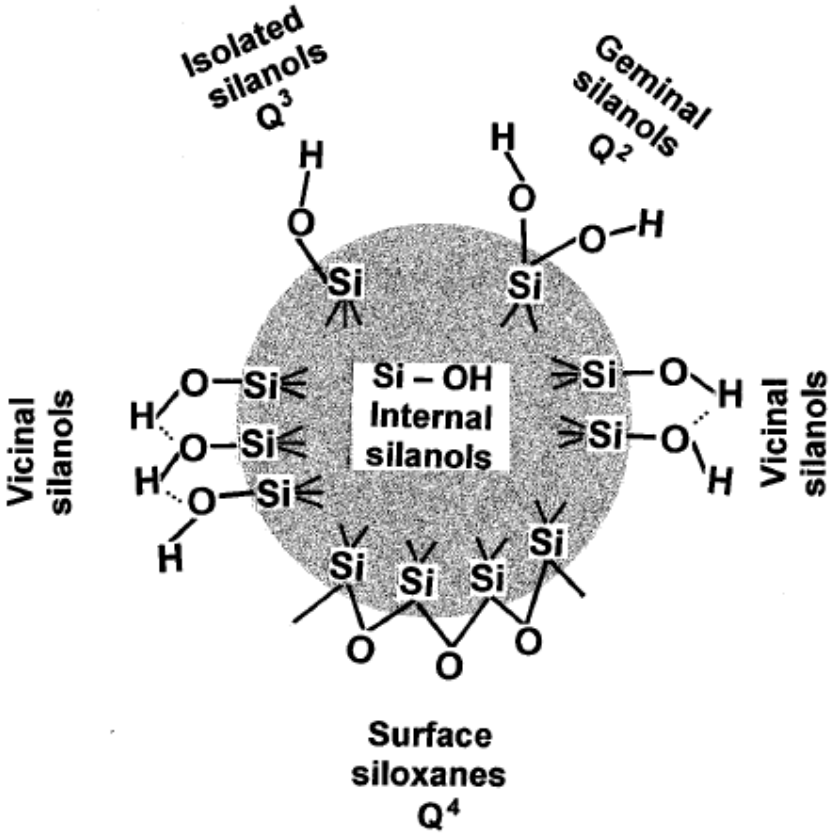

Fig. 1. 6. Various type of silanol groups on SiO_2 [10].

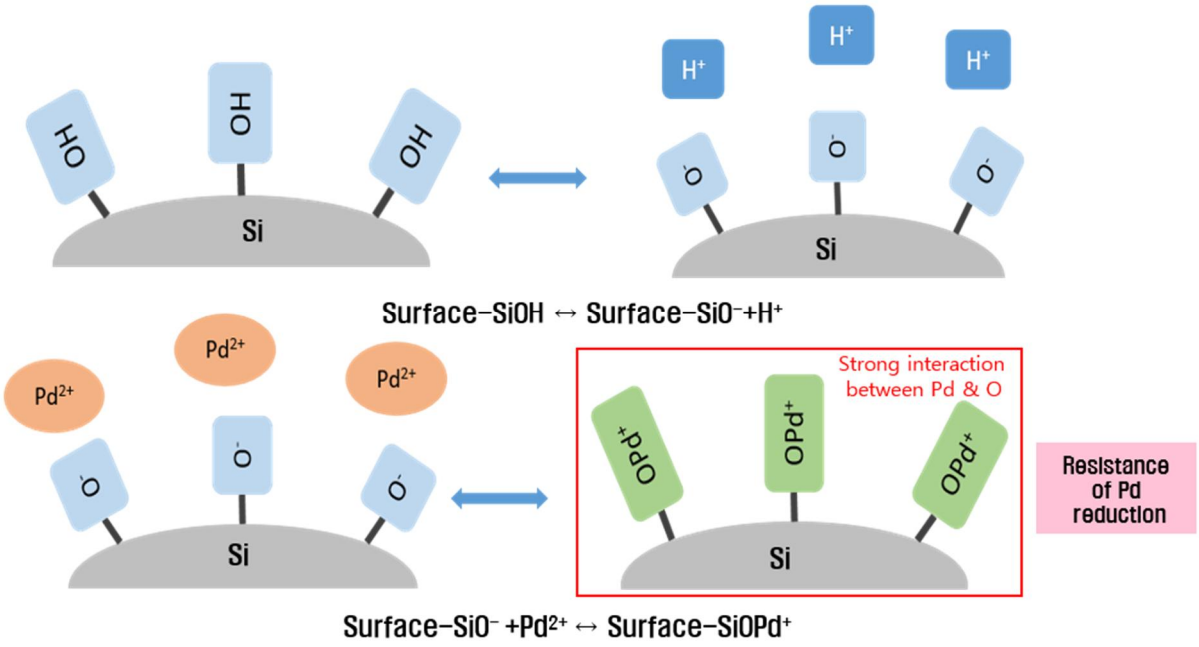

Fig. 1. 7. Mechanism of interaction between silanol groups and palladium ion.

1.3. Activity of prepared catalyst

1.3.1. Catalytic hydrogenation

Hydrogenation reactions are used in a variety of chemical processes, from large-scale refinery industries to small-scale batch processes. Metal catalyzed hydrogenation belongs to the most important transformations in chemical industrial and is a key technology for the manufacture of life science products. For example, during the hydrogenation reaction of a compound having two or more functional groups that can be hydrogenated, it is not easy to hydrogenate selectively only specific functional groups. This is because all the functional groups can be hydrogenated by the activated hydrogen. At this time, when a catalyst having an appropriate kind and activity is used, only a desired specific functional group can be selectively reacted [15].

In addition, the catalyst can greatly increase the reaction efficiency by controlling the activation energy. The rate of elementary reaction is determined by the pre-exponential factor which is in the Arrhenius equation, an empirical relationship between temperature and rate coefficient and activation energy which is the resistance of the chemical reaction. Although the value of the pre-exponential factor varies depending on the reaction, the difference is not so significant, and has little effect on the reaction rate. On the other hand, the activation energy represented by the exponential function greatly affects the reaction rate. Therefore, the rate of chemical reaction is generally compared with the activation energy.

Activation energy is the energy which must be available to a chemical system with potential reactants to result in a chemical reaction. Activation energy may also be defined as the minimum energy required to start a chemical reaction. Therefore when the activation energy is small, the chemical bond can be easily decomposed of generated,

and reaction rate increase. while when the activation energy is large, the reaction is slow because it requires a lot of energy. In order to increase the efficiency of the chemical reaction, it is necessary to reduce the activation energy which is a resistance value for suppressing the progress of the reaction. The catalyst can control the activation energy so that the hydrogenation reaction can proceed rapidly at lower temperatures and pressures than the existing reaction conditions [16].

1.3.2. Hydrogenation of D-glucose

In this study, catalytic activity was confirmed by hydrogenation of D-glucose into D-sorbitol. D-sorbitol is the sugar alcohol with the most widespread uses in food industry, personal care products, cosmetics, medical and industrial applications. Especially, sorbitol has been applied as sweetener in ``sugar free'' food products intended for diabetics. Even today, despite the major contribution of synthetic sweeteners such as aspartame, sorbitol is still frequently applied as sweetener in all kinds of food products [17]. Furthermore, sorbitol is applied as starting material for vitamin C synthesis, ethylene glycol, and glycerol, etc [18].

Although the conversion of D-glucose to D-sorbitol appears simple, in reality, a side reaction can occur instead of conversion into sorbitol. For example, D-glucose can be isomerized to D-fructose by the Lobry de Bruyn-Alberda-van Ekenstein reaction [18, 19]. Generally , Ni-based catalysts are used for catalytic hydrogenation of glucose into sorbitol [21]. However, the Raney Ni type of catalysts can be deactivated due to loss of active Ni surface by sintering, leaching of Ni and promoter metal and poisoning of the active Ni surface by organic species [22]. As alternative to Ni based catalysts, supported noble metals, such as platinum (Pt), rhodium (Rh), palladium (Pd) and ruthenium (Ru), have been also studied in glucose hydrogenation [23].

The glucose hydrogenation activity of catalysts depends on metal dispersion of Pd. Thus, D-glucose transformation into D-sorbitol are studied, in order to gain further understanding of the role of palladium dispersion in D-glucose hydrogenation, respectively. Linking the best results from hydrolysis and hydrogenation steps, it will be possible to choose the most appropriate catalytic system for further one-pot hydrogenation.

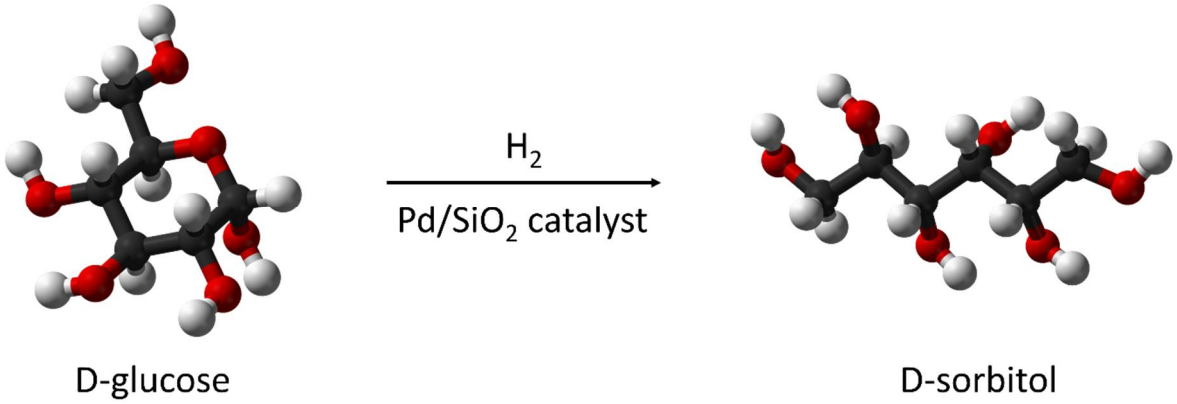

Fig. 1. 8. Hydrogenation of D-glucose.

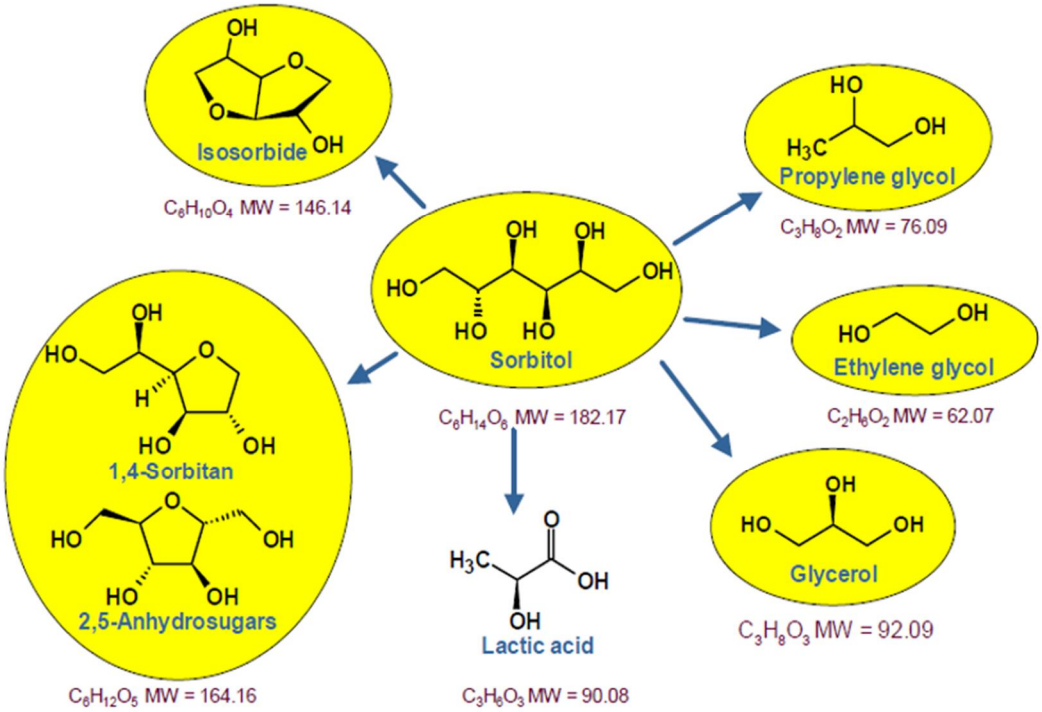

Fig. 1. 9. Sorbitol chemistry to derivatives [18].

2. Experimental

2.1. Preparation of Pd/SiO_2 using the ordered mesoporous silica (OMSs)

2.1.1. Chemicals

Tetraethoxysilane (TEOS) ($Si(OC_2H_5)_4$, 98%, Sigma Aldrich) was employed as precursor, with n-Hexa-decyltrimethylammonium bromide (CTAB) ($CH_3(CH)_{15}NBr(CH_3)_3$, 98%, Sigma Aldrich), Dodecylamin (DDA) ($CH_3(CH_2)_{10}CH_2NH_2$, 98%, Sigma Aldrich), Poly(ethylene glycol)-block-poly(propylene glycol)-block-poly(ethylene glycol) (P123, Sigma Aldrich), Hydrochloric acid (HCl, 38%, Sigma Aldrich), Ammonium hydroxide (NH_4OH, 25-28%, Dae Jung), Ethanol (C_2H_6O, 99.5%, Dae Jung) were used during catalyst preparation.

2.1.2. Ordered mesoporous silicas (OMSs)

2.1.2.1. SBA-15

Synthesis of mesoporous silica, SBA-15, has been carried out using a hydrothermal method. First, P123 (8.79 g) was dissolved in 66 mL of H_2O and then 264 mL of HCl (2 M) were added to the solution. The mixture was vigorously stirred at 40 ℃ for 1 h. TEOS (20 mL) was added to the surfactant solution resulting in a reaction mixture and stirred for 2 h. after then the solution was aged at 35 ℃ for 24 h and then at 80 ℃ for 48h. The final solid product was recovered by filtration, washed with water and dried at 105 ℃ for 12h and calcined 550 ℃ for 6h. The overall flow chart for the synthesis of SBA-15 by hydrothermal method is given in Fig. 2. 1.

2.1.2.2. MCM-48

MCM-48 has been carried out using a conventional hydrothermal pathway similar to the procedure described by Schumacher et al. [24]. 2.4 g n-Hexadecyltrimethyl-ammonium bromide template ($CH_3(CH_2)_{15}N(Br)(CH_3)_3$) was dissolved in the mixed solution of 42 mL of distilled water, 13 mL of aqueous ammonia and 13 mL ethanol. The mixture was stirred for 15 min and then 4.26 mL of TEOS were dropwise at 0.5 mL/min. The solution was stirred continuously for 18 h. The final solid product was recovered by filtration, washed with water and dried at 105 ℃ for 12 h and calcined 550 ℃ overnight. The overall flow chart for the synthesis of MCM-48 by hydrothermal method is given in Fig. 2. 1.

2.1.2.3. HMS

Hexagonal molecular sieves (HMS) were prepared via a hydrothermal synthesis method [25]. First, 4.15 g of DDA, 55 mL ethanol and 75 mL of distilled water were vigorously stirred for 15 min. has been carried out using a hydrothermal method. TEOS (20 mL) were dropwise at 0.5 mL/min. The surfactant solution resulting in a reaction mixture with a ratio is TEOS : DDA : EtOH : H_2O of 4 : 1 : 41.5 : 170. After then, the solution was aged at 55 ℃ for 20 h. The final solid product was recovered by filtration, washed with water and dried at 105 ℃ for 12h calcined 550 ℃ for 6h. The overall flow chart for the synthesis of HMS by hydrothermal method is given in Fig. 2. 1.

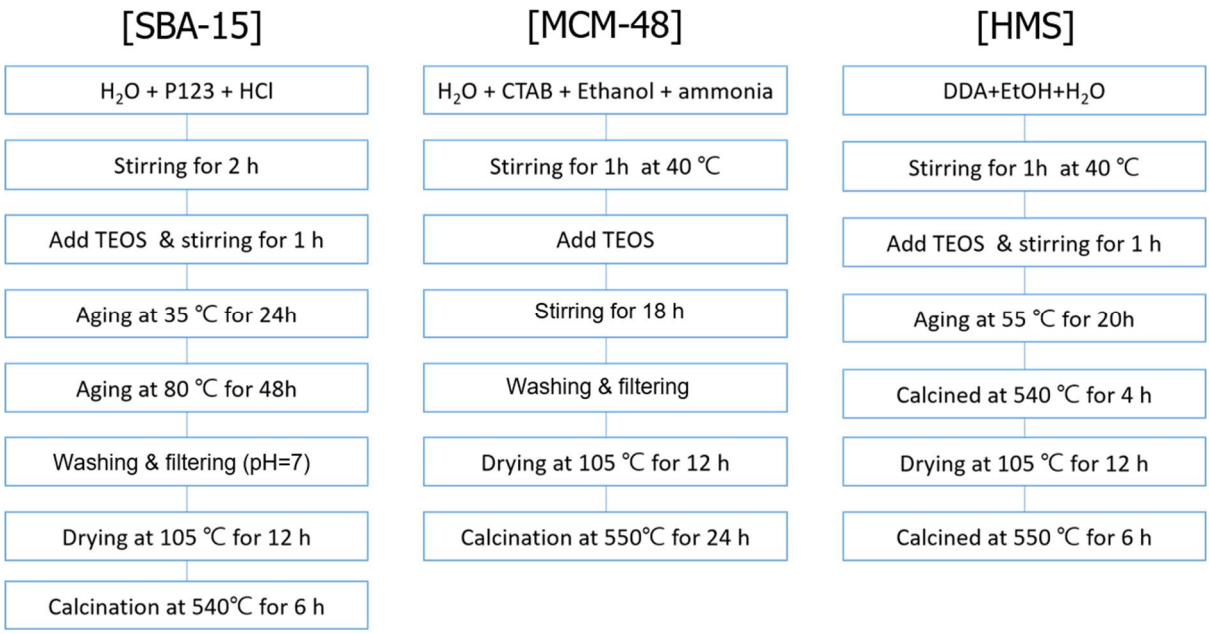

Fig. 2. 1. Preparation of ordered mesoporous silicas (OMSs).

2.1.3. Pd catalysts supported on OMSs

The Pd/OMS catalysts were prepared using an ion-exchange method. A 0.1 M solution of PdCl2 in HCl was employed as the metal precursor, and a portion of this solution was added to a 1 mM solution of sodium tartrate at 5 °C. The desired quantity of pretreated OMS was then dispersed into this solution and the solution pH was adjusted to 6.0 by the addition of an aqueous NaOH solution. After stirring for 2 h, a freshly prepared 0.35 M solution of sodium borohydride was added to the above solution then stirred at 5 °C for 2 h to reduce the Pd salts to Pd metal particles. These particles were then isolated by filtration and washed with distilled water until a pH of 5–6 was reached. Finally, the particles were dried at 110℃ over 12 h. The overall flow chart for the preparation of Pd/OMS catalysts by ion-exchange method is given in Fig. 2. 2.

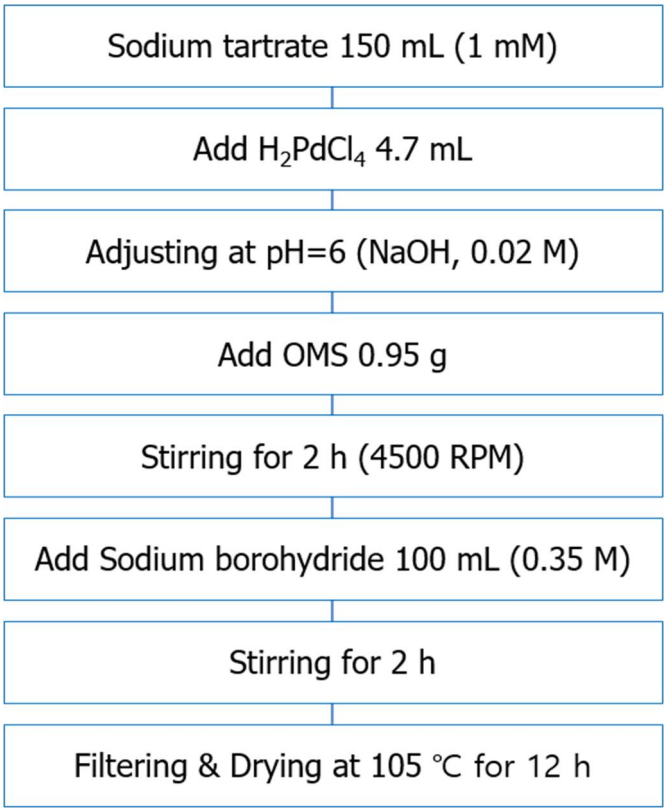

Fig. 2. 2. Preparation of Pd/OMS catalyst.

2.1.4. Characterization of supports and catalysts

Several physical and chemical techniques were employed to characterize supported Pd catalysts. The specific surface areas and porous structures of the pretreated supports were examined by nitrogen adsorption-desorption (ASAP2020 Surface Area Analyzer, USA) at −196 °C. The samples were degassed under vacuum at 150 °C for 4 h prior to measurement. In order to determine the specific area, nitrogen adsorption, Brunauer-Emmett-Teller (BET) equation isapplied, and the total pore volume and pore size was calculated by Barrett-Joyner-Halenda (BJH) method. X-ray diffraction (XRD, D/MAX 2500-V/PC, Rigaku, Japan) was used to characterize the crystal structures of OMS supports and the prepared catalysts in the 2θ range of 1–10° and 10–90°. Field-emission transmission electron microscopy (FE-TEM, JSM-6700F, JEOL, Japan) was used to determine the pore structures of OMS support, particle sizes and distributions of the deposited Pd. while the Pd dispersions were evaluated by examining the CO adsorption capacity using a pulse technique (CO-chemisorption, AutoChem 2920, Micromeritics Instruments Corp., USA) assuming a Pd:CO adsorption ratio of 2:1.

2.2. Preparation of Pd/SiO_2 with functional groups modification

2.2.1. Chemicals

Silicon dioxide (SiO_2, 99.5%, Sigma Aldrich) was employed as the support, and ammonium hydroxide (ammonia water) (NH_4OH, 25-28%, Dae Jung) was used for pretreatment. Also sodium tartrate (Na2C4H4O6, ≥99%, Sigma Aldrich), Hydrochloric acid (HCl, 38%, Sigma Aldrich), Palladium chloride ($PdCl_2$, ≥99%, Sigma Aldrich), Sodium borohydride (NaBH4, 95%, Sigma Aldrich), Sodium hydroxide (NaOH, ≥98%, Sigma Aldrich) were used for catalyst preparation.

2.2.2. Liquid modification of functional groups by ammonia water

The concentration of surface functional groups may be modified by ammonia water treatment. 2 g commercial SiO_2 (SiO_2_N) was placed along with a medium (10 vol.% ammonia water) in a Teflon lined autoclave. The reaction temperature was raised 150 to 250 ℃ ramping at 10 ℃/min and kept at this temperature for 2 h with stirring 300 rpm. Then the mixture was filtrated and dried overnight at 105 ℃. The obtained supports were labelled as follows: SiO_2_A150, SiO_2_A200 and SiO_2_A250 respectively, where the number indicates the treatment temperature. The overall flow chart for the liquid modification of functional groups is given in Fig. 2. 3.

2.2.3. Dry modification of functional groups by thermal treatment

The concentration of surface functional groups may be modified by thermal treatment. The SiO_2 supports were calcined at the desired temperature between 100 and 1100 ℃ for 4hr with a heating rate of 5℃/min, and the obtained supports were labelled as follows: SiO_2_100, SiO_2_300, SiO_2_500, SiO_2_700, SiO_2_900, and SiO_2_1100, where the number indicates the calcination temperature.

2.2.4. Preparation of Pd/SiO_2 catalyst with functional groups modification

The Pd/SiO_2 catalysts with functional groups modification were prepared using an ion-exchange method. This method of preparation chosen a high dispersion of the metal on the support, because the precursor is strongly adsorbed on the surface of the support. In addition in this method, It is possible to know how the functional group affects the reduction of the palladium ion, during the preparation of catalysts.

A 0.1 M solution of $PdCl_2$ in HCl was employed as the metal precursor, and a portion of this solution was added to a 1 mM solution of sodium tartrate at 5 °C. The desired quantity of pretreated SiO_2 was then dispersed into this solution and the solution pH was adjusted to 6.0 by the addition of an aqueous NaOH solution. After stirring for 2 h, a freshly prepared 0.35 M solution of sodium borohydride was added to the above solution then stirred at 5 °C for 2 h to reduce the Pd salts to Pd metal particles. These particles were then isolated by filtration and washed with distilled water until a pH of 5–6 was reached. Finally, the particles were dried at 110℃ over 12 h. The overall flow chart for preparation of Pd/SiO_2 with functional groups modification is shown in Fig. 2. 4.

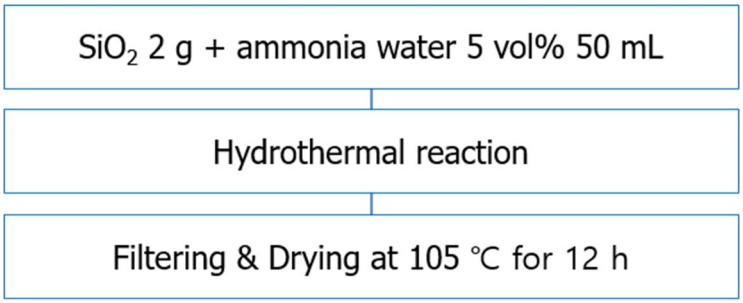

Fig. 2. 3. Preparation of SiO_2 by ammonia water.

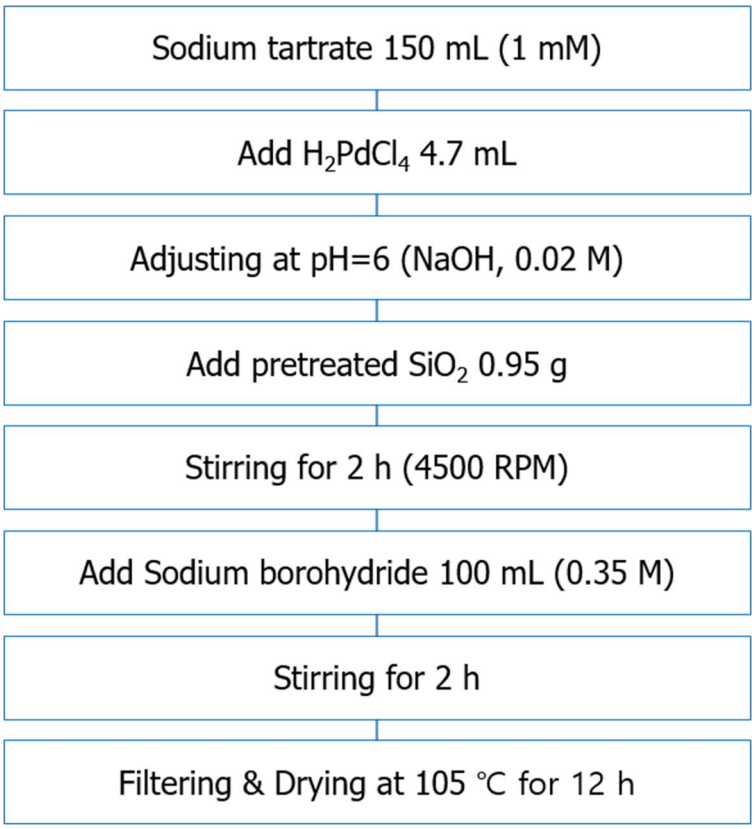

Fig. 2. 4. Preparation of Pd/SiO_2 with functional groups modification.

2.2.5. Characterization of supports and catalysts

The specific surface areas and porous structures of the pretreated supports were examined by nitrogen adsorption-desorption (ASAP2020 Surface Area Analyzer, USA) at −196 °C. The samples were degassed under vacuum at 150 °C for 4 h prior to measurement. The silanol group concentration was obtained by Fourier transform infrared spectroscopy (FT-IR, Nicolet 6700, Thermo Fisher, USA) and ammonia temperature-programmed desorption measurements (NH3-TPD, AutoChem 2920, Micromeritics Instruments Corp., USA). X-ray diffraction (XRD, D/MAX 2500 V PC, Rigaku, Japan) was used to characterize the crystal structures of the pretreated supports and the prepared catalysts in the 2θ range of 10–90°. Field-emission transmission electron microscopy (FE-TEM, JSM-6700F, JEOL, Japan) was used to determine the particle sizes and distributions of the deposited Pd. The H_2 uptake during the reduction process was measured by temperature-programmed reduction with hydrogen (H2-TPR, AutoChem 2920, Micromeritics Instruments Corp., USA), while the Pd dispersions were evaluated by examining the CO adsorption capacity using a pulse technique (CO-chemisorption, AutoChem 2920, Micromeritics Instruments Corp., USA) assuming a Pd : CO adsorption ratio of 2:1.

2.3. Liquid phase hydrogenation of D-glucose

2.3.1. Chemicals

D-glucose ($C_6H_{12}O_6$, ≥99.5%) were obtained from Sigma-Aldrich. Standard materials of D-sorbitol ($C_6H_{14}O_6$, ≥98%), fructose ($C_6H_{12}O_6$, ≥99%), glycerol ($C_3H_{12}O_3$, ≥99%), were obtained from Sigma-Aldrich with analytical reagent grade. Nitrogen and hydrogen gas with minimum state purity of 99.0% was obtained from DeokYang.

All chemicals were extra pure reagent grade and used as obtained without further purification. Deionized water was prepared with an ion-exchange system.

2.3.2. Procedure of hydrogenation of D-glucose

The reaction was performed in batch in a 100 mL capacity stainless steel (Material:316SS) auto clave. The reactor was equipped with an electrically heated jacket, a turbine agitator and variable speed magnetic drive. The temperature and the speed of agitation were controlled by controller. The gas inlet, gas release valve, cooling water feed line and pressure gauge situated on top of the reaction vessel.

In order to optimize the reaction parameters for the hydrogenation of D-glucose, experiments were tested with different reaction time and H_2 pressure under the conditions of reaction temperature 120℃, stirring speed 1000 rpm and using 0.15g catalyst. And then the hydrogenation using the catalysts having different metal dispersions proceeded under optimized reaction conditions.

The hydrogenation reaction was performed by 60 mL of glucose solution (10 g/L) and charging 150 mg of the prepared catalysts with different metal dispersion of Pd. All the catalytic tests were performed at 120 °C and 2.5 MPa of pure hydrogen during 360 min [20].

First, the reactor was purged with N_2 for leak-proof under nitrogen pressure. Then hydrogen was introduced to purge out nitrogen to 1.0 MPa. After the reaction temperature set, the pressure was raised to desired value, 2.5 MPa. The detailed process and reactor for production of sorbitol was shown in Fig. 2. 5. and Fig. 2. 6.

The product distribution was analyzed by HPLC (Agilent, HPLC series 1200) equipped with RI detection and Hi-Plex Ca (300 * 7.7 mm) column and operated at 80 ℃, eluent water with flow rate of 0.5 mL/min. D-glucose conversions, D-sorbitol yield and selectivity were calculated using Eqs. (2.1)− (2.3)

$$X_{D-gluose}\ (\%) = \frac{mole\ (D-glucose_0) - mole\ (D-glucose_f)}{mole\ (D-glucose_0)} \times 100 \quad (2.1)$$

$$S_{Sorbitol}\ (\%) = \frac{mole\ (Sorbitol)}{mole\ (D-Glucose_0) - mole\ (D-Glucose_f)} \times 100 \quad (2.2)$$

$$Y_{Sorbitol}\ (\%) = \frac{mole\ (Sorbitol)}{mole\ (D-Glucose_0)} \times 100 = \frac{X \times S}{100} \quad (2.3)$$

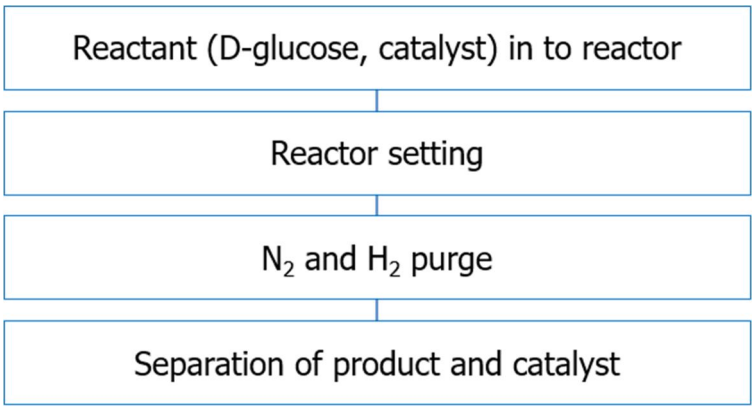

Fig. 2. 5. Procedure of hydrogenation of D-glucose.

Fig. 2. 6. 100 mL autoclave reactor for hydrogenation of D-glucose.

3. Result and discussion

3.1. Pd/SiO_2 using the ordered mesoporous silica (OMSs)

3.1.1. Pore properties of synthesized OMSs

Nitrogen adsorption-desorption is one of the most employed methods of characterization of porous materials. Fig. 3. 1. show the N_2 adsorption-desorption isotherms of the samples, and textural parameters calculated from the adsorption isotherms are collected in Table 1. All Prepared OMS has very large specific surface area, over 500 m^2/g. This results suggest that all supports have very well-ordered mesopores.

All samples have hysteresis loop which is meaning a characteristic of meso pore structure. According to IUPAC classification [8], Fig. 3. 1. (a), (b) have well-defined H1-type hysteresis loop. This hysteresis of SBA-15 is associated with porous materials consisting of well-defined cylindrical-like pore channels [26]. And Fig. 3. 1. (c) presents H4-type hysteresis loop associated with narrow slit pores. And according to geometrical effect and Kelvin equation, the area of hysteresis loop is in direct proportion to number of pore. So that the volume of porosity in the sequence of SBA-15 > MCM-48 > HMS is increased and all supports has a narrow pore size distribution with the average pore size of under 5 nm. This results are in good agreement with the pore volume and pore diameter in Table 3. 1 and Fig. 3. 2. [27].

Fig. 3. 3. shows the low-angle XRD patterns of OMS. All samples exhibited XRD patterns with very intense diffraction peak. From Fig. 3. 3. (a), SBA-15 has very intense diffraction peak indexed to the (100) plane, and two weak intense peaks indexed to the (110) and (200) planes, which caused by a typical hexagonal mesopore structure [19, 20].

And exhibits tree main diffraction peaks at 2-5˚, that can be assigned to (211), (220)

and (332) planes in Fig. 3. 3. (b) [28]. Also the characteristic peak of (100) plane of HMS-type materials at 2–3° is detected over (Fig. 3. 3. (c)) [29].

The mesoporous structure of the materials was also investigated with FE-TEM images. Fig. 3. 4. material grains with a regular array of mesoporous. Observation along a direction close to the pore axis revealed a prismatic structure with a hexagonal cross-section of plane group symmetry. The observed pore diameter (D ~ 5 nm) are in a reasonable agreement with the value from the low angle XRD and N_2 adsorption measurements.

Table. 3. 1 Physical properties of OMSs by nitrogen adsorption and desorption

Supports	Specific surface area (m^2/g)	Pore volume (cm^3/g)	Pore size (nm)
SBA-15	829.80	0.951	5.76
MCM-48	532.71	0.593	4.99
HMS	689.67	0.663	3.16

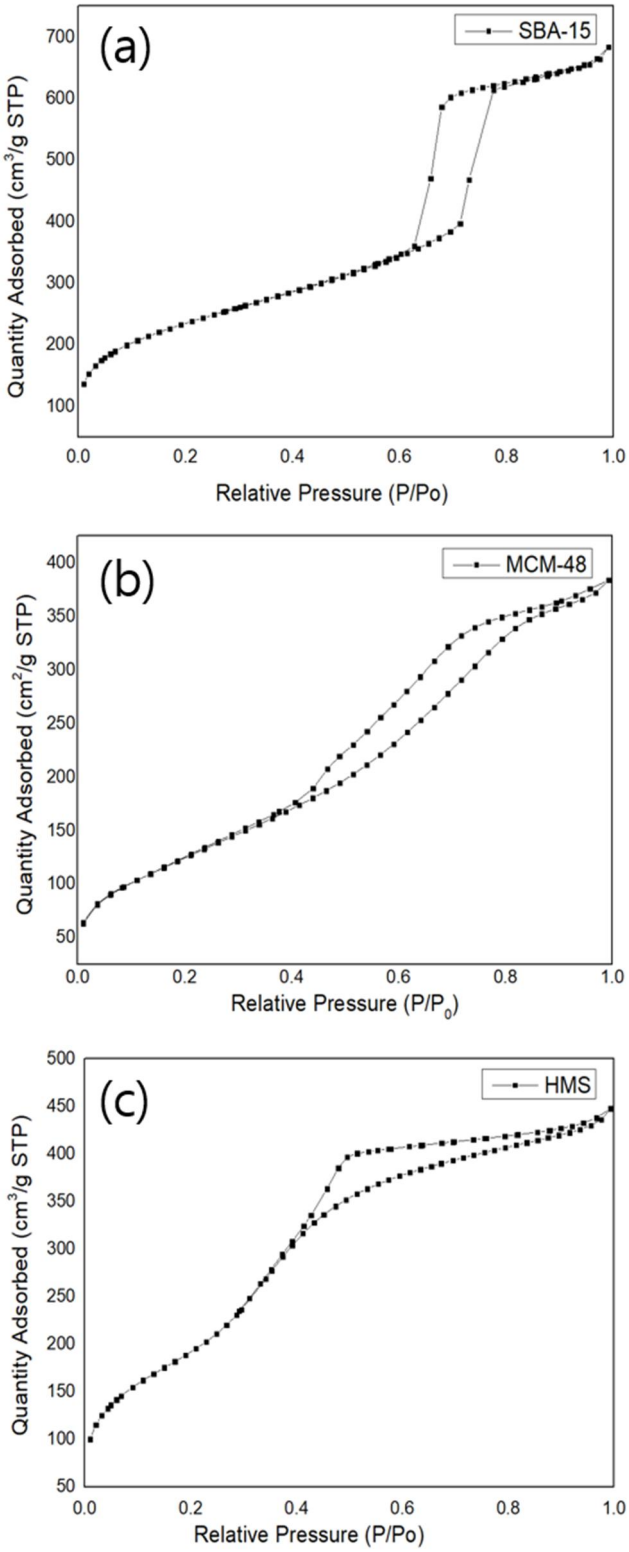

Fig. 3. 1. Nitrogen adsorption and desorption isotherm of OMSs;
(a) SBA-15, (b) MCM-48 and (c) HMS.

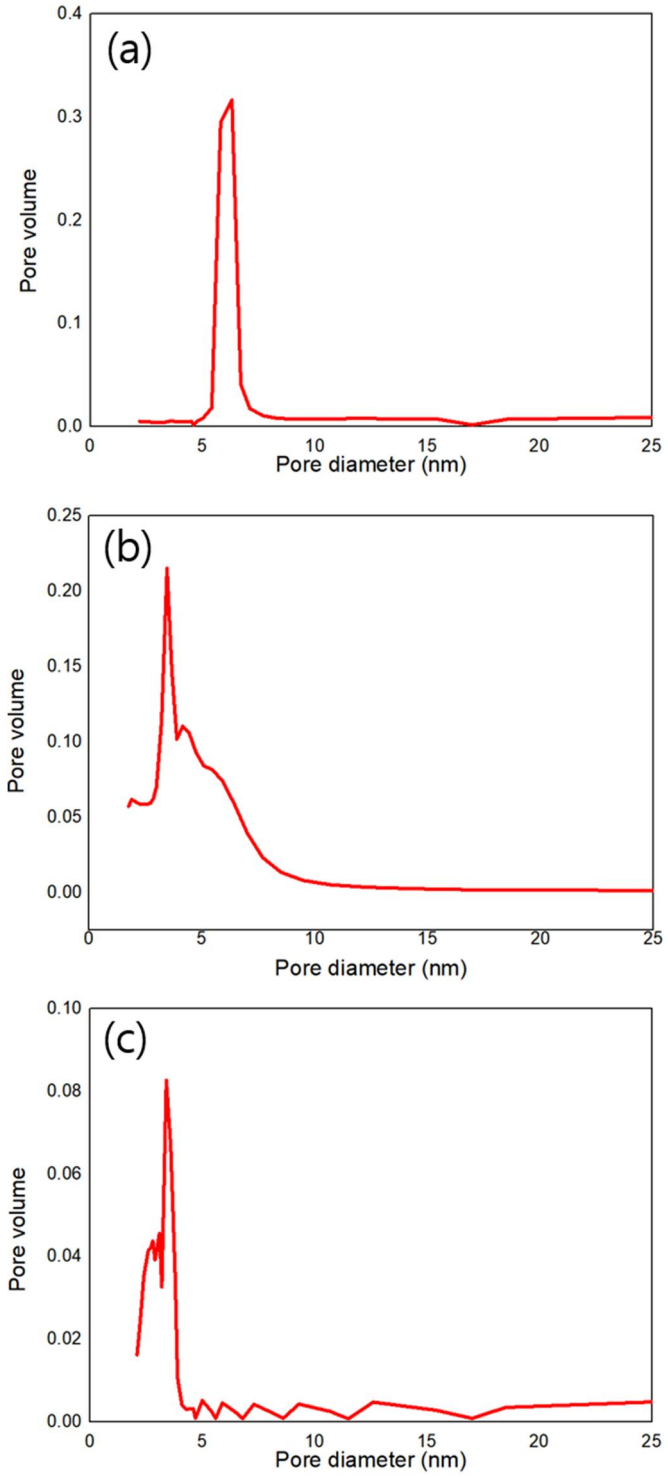

Fig. 3. 2. BJH pore-size distributions of OMSs; (a) SBA-15, (b) MCM-48 and (c) HMS.

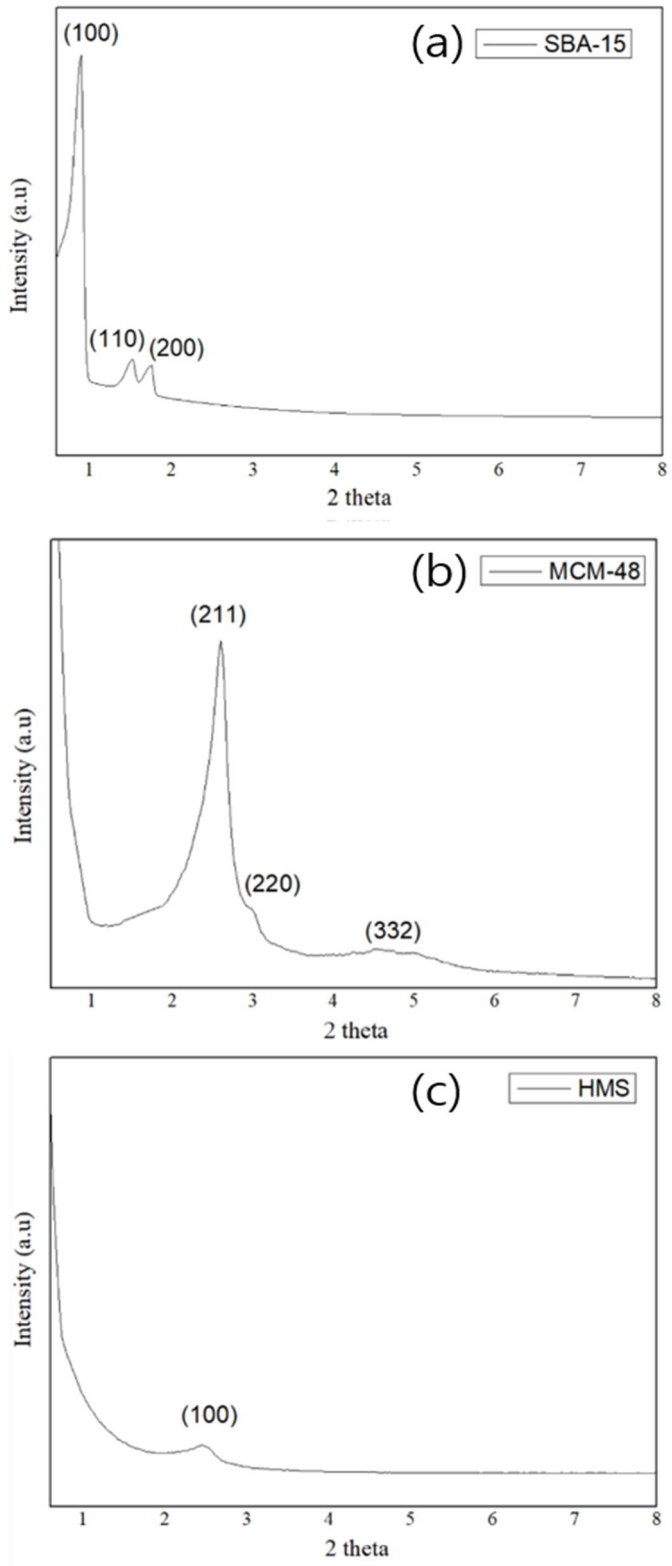

Fig. 3. 3. Low angle XRD patterns of OMSs; (a) SBA-15, (b) MCM-48 and (c) HMS.

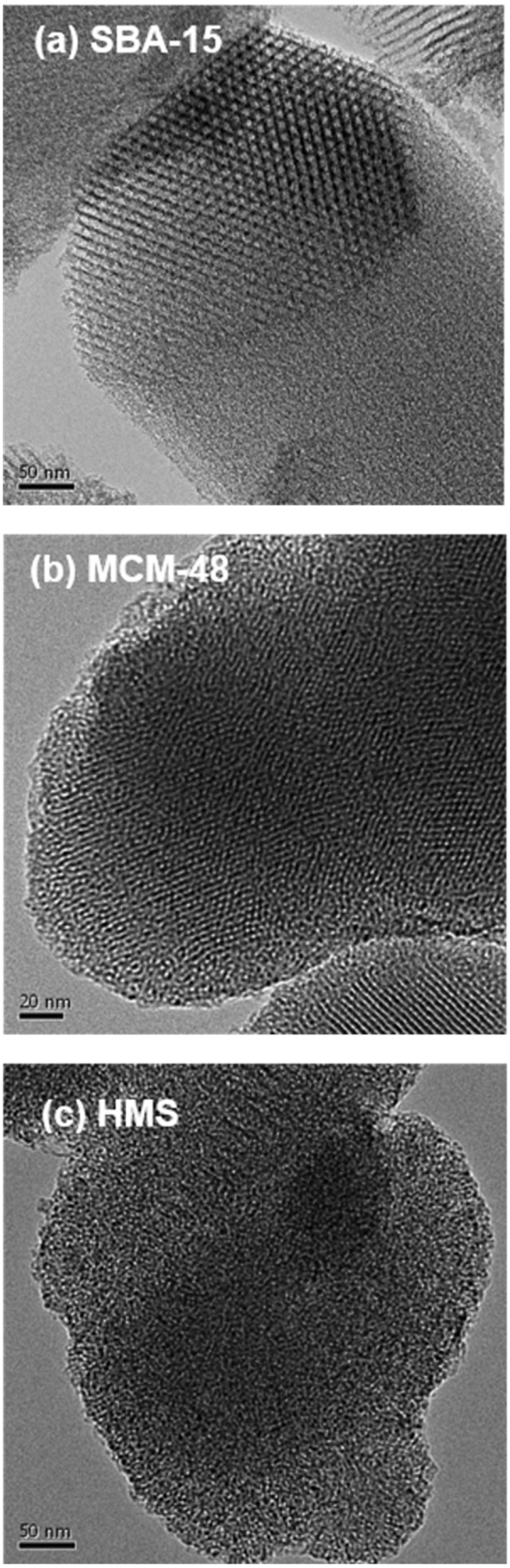

Fig. 3. 4. FE-TEM image of OMSs; (a) SBA-15, (b) MCM-48 and (c) HMS.

3.1.2. Pd/SiO_2 using the ordered mesoporous silicas (OMSs)

The specific surface areas and pore propertis are summarized in Table 3. 2. A slight decrease of specific surface area and pore volume were observed compared with supports only. It can be seen that the Pd particle deposited on the supports affected these decreases, because Pd particles blocked the pore of supports [1].

Table 3. 3 show the metal dispersion of Pd by CO-chemisorption results. It can be seen that all three catalysts have low metal dispersion. This is because the silica has a low metal interaction and the OMSs have so stable surface state. So that the palladium partcle were not distributed on the OMS supports evenly and reduced to aggregated state. Among the three Pd / HMS dispersions, Pd / HMS has the lowest metal dispersion. It seems that the Pd particles are not uniformly dispersed among the pores because of the narrow slit-like pore with an average pore diameter of only 3 nm.

XRD profiles were performed to identify the crystalline structures of the prepared Pd/SiO_2 (Fig. 3. 5.). All catalysts showed broad peaks at $2\Theta = 22.21^{\circ}$, indicating the amorphous SiO_2 peak. And also, The strong diffraction peaks appear in the all catalysts at 39.92°, 46.43° and 67.77° which could be ascribed to characteristic diffraction peaks of Pd. Comparing the Pd peak of Pd/HMS, catalysts which is used the others supports have broad peaks of Pd. Pd/SBA-15 has the broadest Pd peak. It can be suggested that the Pd particle on the Pd/SBA-15 dispersed evenly compared with the other prepared catalysts. Because the broadness of the XRD patterns is associated with small crystallite sizes of Pd [30]. These results accord closely with CO-chemisoprtion results.

Fig. 3. 6. is presented the Pd particle size and metal dispersion by FE-TEM. Pd particles of all Pd/OMS were well reduced to 2-5 nm in size, but they were terribly aggregated each other. This results are in good agreement with CO-chemisorption and XRD results.

Table. 3. 2 Textural properties of Pd/OMS catalysts

Support	Specific surface area (m^2/g)	Pore volume (cm^3/g)	Pore size (nm)
Pd/SBA-15	786.25	0.894	5.14
Pd/MCM-48	467.97	0.568	4.41
Pd/HMS	609.73	0.612	2.56

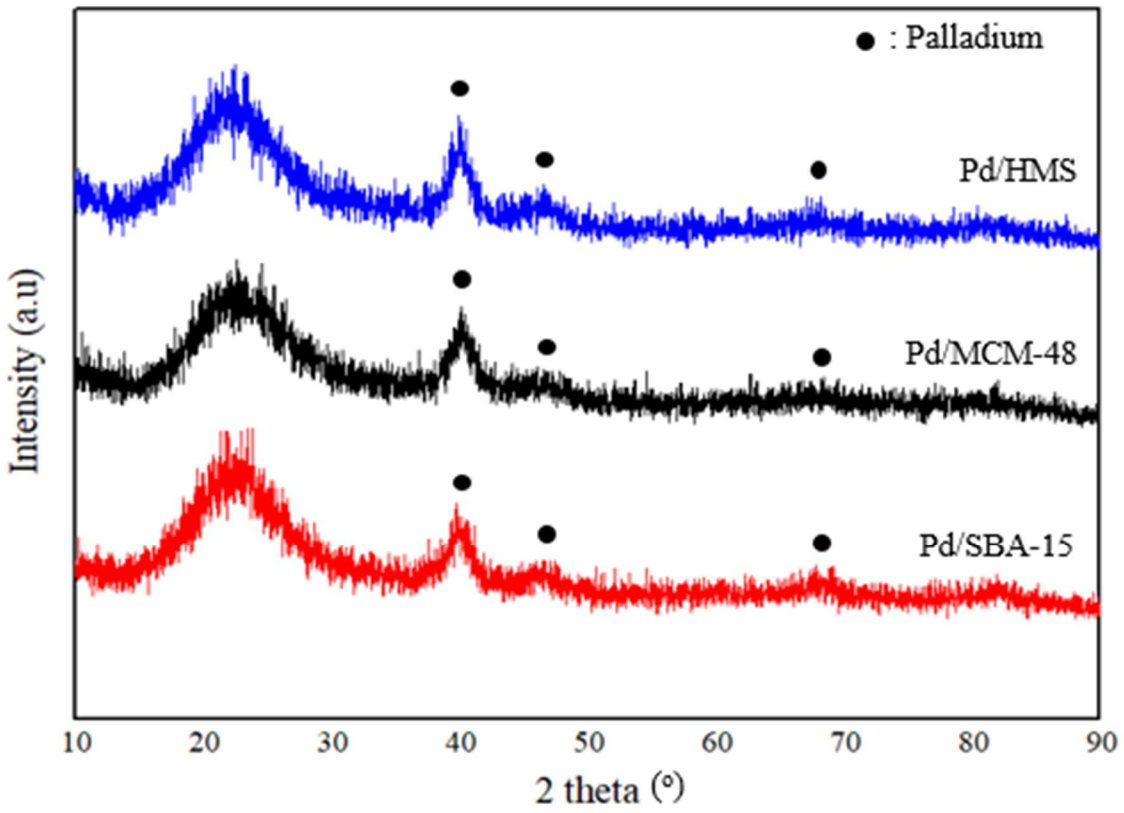

Fig. 3. 5. XRD patterns of Pd/OMS catalysts.

Table. 3. 3 CO-chemisorption results of Pd/OMS catalysts

Catalysts	Metal dispersion (%)	Metallic surface area (m^2/g metal)	CO gas adsorption (mmol/g)
Pd/SBA-15	6.18	0.014	27.51
Pd/MCM-48	5.31	0.012	23.67
Pd/HMS	5.07	0.011	22.60

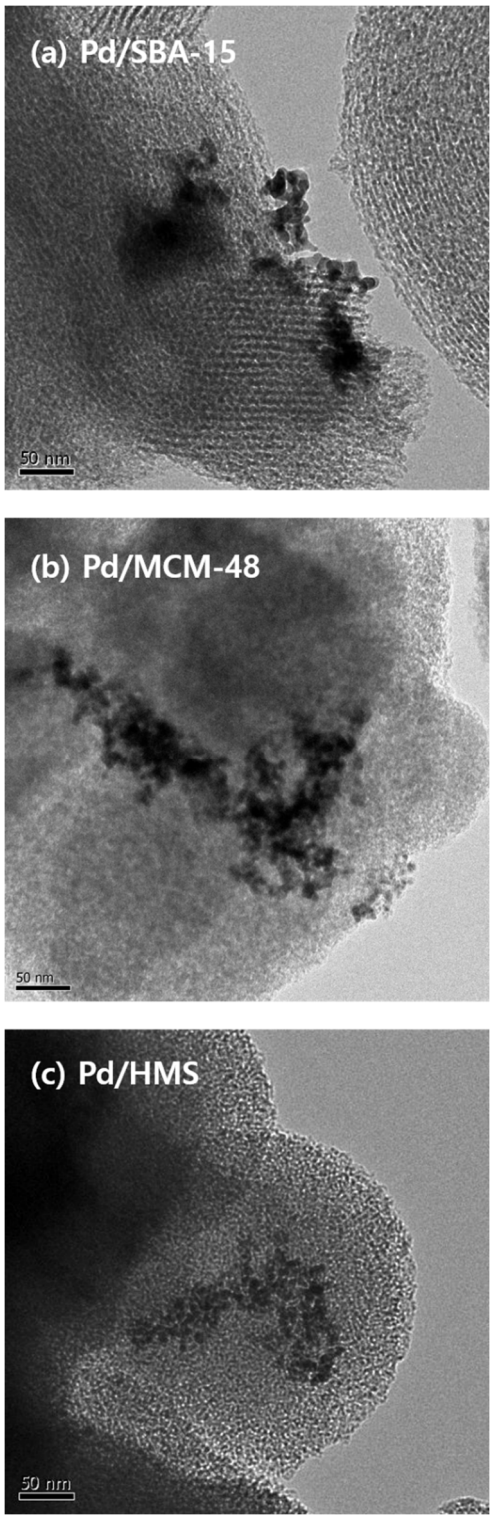

Fig. 3. 6. FE-TEM images of Pd/OMS catalysts;
(a) Pd/SBA-15, (b) Pd/MCM-48, (c) Pd/HMS.

3.2. Pd/SiO_2 with functional groups modification

3.2.1. Liquid modification of functional groups by Ammonia water

N_2-physisiorption analysis was performed to investigate the effect of ammonia treatment on the pore structure of the support. The BET surface areas, pore volumes and average pore diameters of the pretreaed supports are listed up in Table 3. 4. The specific surface area of the support decreases with increasing the pretreatment temperature from 148.97 m^2/g to 59.86 m^2/g. This results can be suggested that the silica structure was collapsed and dissolving by the ammonia water treatment in increasing temperature [14]. Because the solubility of amorphous silica increases significantly with increase of pH, as illustrated in Fig. 3. 7. Aggregates composed of amorphous or poorly crystalline silica will tend to dissolve more readily in the inherently high-pH pore solution in concrete [31].

The effect of ammonia water treatment on modification of functional groups (silanol groups) is investigated by FT-IR. The spectra of the pretreated SiO_2 support are presented in Fig. 3. 8. There are the Si-O-Si stretching and vending vibration at 1150, 800 and 480 cm^{-1}, and a small absorption band at 960 cm^{-1} is observed on the support, which is ascribed to the symmetric stretching vibration of –OH group [14]. Comparing the untreated silica support (SiO_2_N), there is an obvious decrease in the intensity of silanol group peak with increasing pretreatment temperature. The intensity of the Si-OH stretching vibration decreased in the order SiO_2_N > SiO_2_A150 > SiO_2_A200 > SiO_2_A250, implying that is the order of the surface silanol concentration [13]. As observed in FT-IR, the silanol group was almost disappeared over the pretreatment temperature 200 ˚C. It is reason that high temperature increases the reactivity between the ammonia and Silica.

Fig. 3. 9. shows the XRD profiles of the pretreated SiO_2 supports. All catalysts showed broad peaks at $2\Theta = 22.21^{\circ}$, indicating the amorphous SiO_2 peak. The XRD patterns indicate that not only untreated SiO_2 but also all pretreated SiO_2 retain the amorphous phase. This phenomenon indicates that the ammonia water pretreatment do not influence the SiO_2 phase.

Table. 3. 4 Textural properties of SiO_2 supports pretreated by ammonia water

Supports	Specific surface area (m^2/g)	Pore volume (cm^3/g)	Pore size (nm)
SiO_2_N	150.23	1.122	38.05
SiO_2 _A150	104.92	0.979	41.58
SiO_2 _A200	79.16	0.245	24.66
SiO_2 _A250	59.86	0.181	18.00

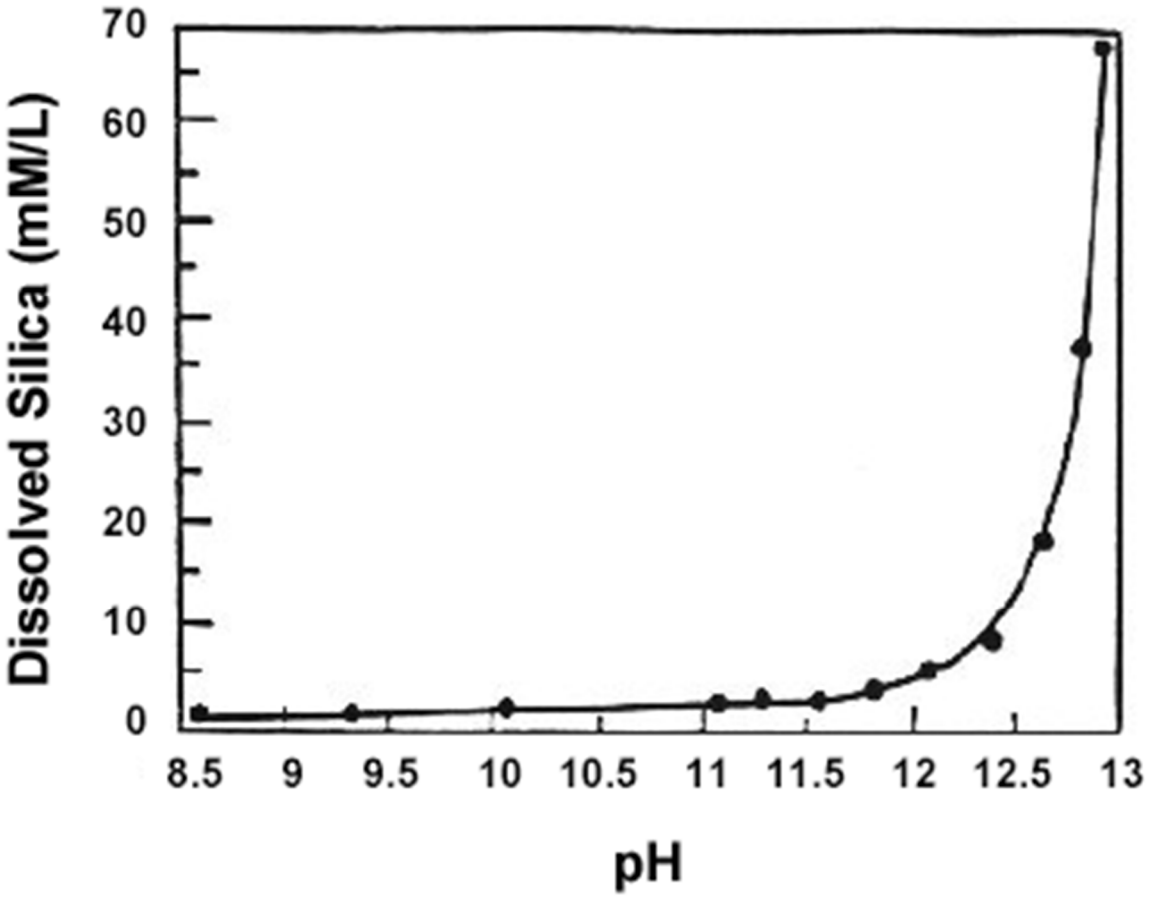

Fig. 3. 7. Effects of pH on Dissolution of Amorphous Silica (Tang and Su-Fen, 1980) [31].

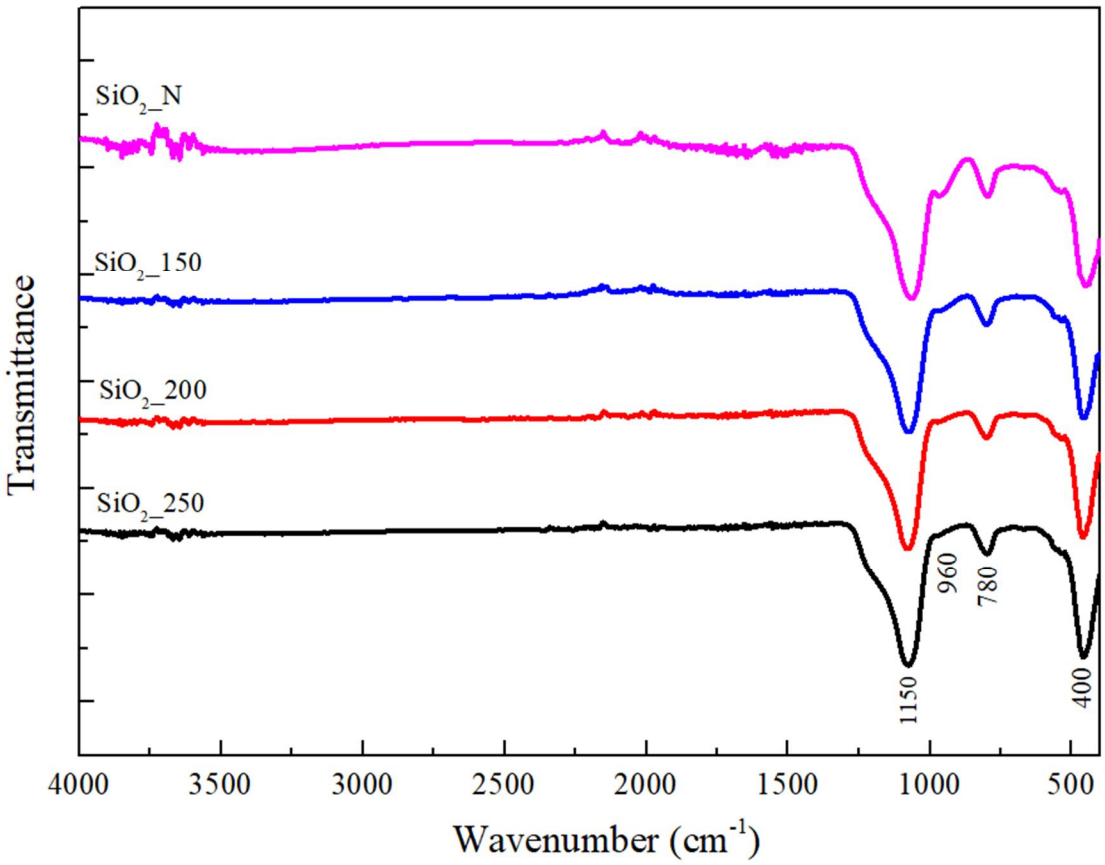

Fig. 3. 8. FT-IR spectra of pretreated SiO_2 support by ammonia water.

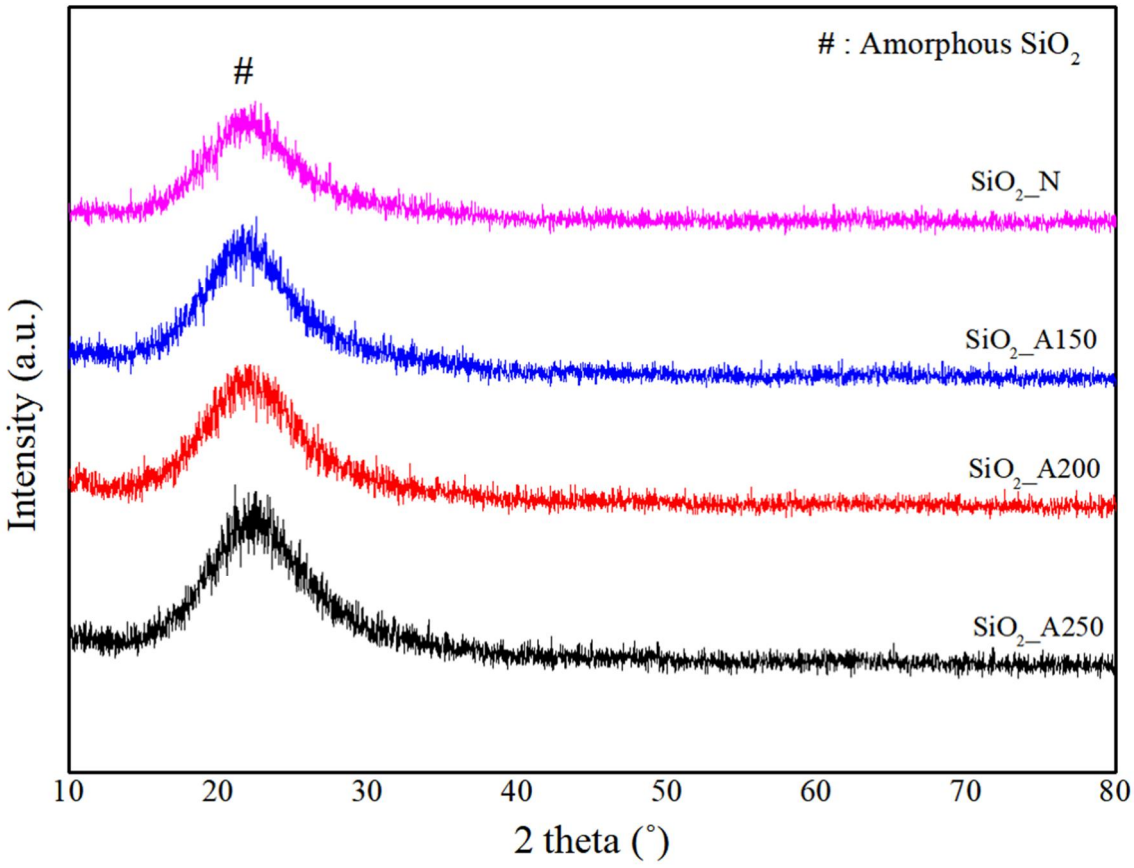

Fig. 3. 9. XRD patterns of pretreated SiO_2 support by ammonia water.

3.2.2. Pd catalyst supported on liquid modified SiO_2

N_2-physisorption was carried out to investigate the effect of the palladium loading on the pore structure of the support. The textural properties of catalysts including BET surface area and pore volume and pore size were shown in Table 3. 5. A slight decrease of specific surface area and pore volume were observed compared with supports only. It can be deduced that the palladium particles block the pores of the support and that the specific surface area and pore volume of the catalyst are reduced [32].

The XRD patterns of the prepared catalysts were presented in Fig. 3. 10. The peak at 2 theta of 40.1, 46.9, 68, and 82.1˚ could be ascribed to characteristic diffraction peaks of crystal Pd. The results of XRD patterns presented the weak Pd peak intensity at the Pd/SiO_2_A200 patterns. It can be suggested that the Pd particle well dispersed compared with the other prepared catalysts. Because the broadness of the XRD patterns is associated with small crystallite sizes of Pd [30].

Table 3. 6 show the metal dispersion of Pd by CO-chemisorption results. The metal dispersion of Pd increased when pretreatment temperature increase up to 200 ˚C, Pd/SiO_2_A200 has the highest Pd dispersion as 8.82%. Combing the results of FT-IR results and N_2 adsorption-desorption, it can be seen that the decline of silanol groups leads a increase of the metal dispersion of Pd. Because the silanol groups caused strong interaction between Pd and Oxygen(O) element which interrupt the reduction of metal, The removal of the silanol groups bring positive influence of metal reducibility [13,14,30]. However, the metal dispersion of Pd/SiO_2_A250 decreased to 4.71% although the intensity gap of silanol group peak between SiO_2_A200 and SiO_2_A250 are minor. This phenomenon can be explained that the decreas of specific surface area have a negative effect on the metal dispersion of Pd/SiO_2_A250.

Fig. 3. 11. is presented the Palladium particle size and metal dispersion by FE-TEM.

It can be verified that the average particle size of Pd is about 2-5 nm. The Pd particle dispersed evenly when it was deposited on support pretreated with ammonia water at 200 ℃ compared with the other Pd catalysts (Fig. 3. 11. (c)). This result can back that the removal of silanol groups lead to increase of the Pd dispersion. However, the SiO_2 support size increased and the Pd particles were agglomerated again at 250 ˚C. Beacaus the low specific area of the SiO_2 support caused by the pretreatment with ammonia has negative impact on high metal dispersion [9].

Table. 3. 5 Textural properties of Pd/SiO_2 catalysts pretreated by ammonia water

Catalysts	Specific surface area (m^2/g)	Pore volume (cm^3/g)	Pore size (nm)
Pd / SiO_2_N	148.97	0.576	19.35
Pd / SiO_2 _A150	102.07	0.494	25.21
Pd / SiO_2 _A200	73.32	0.295	22.12
Pd / SiO_2 _A250	55.75	0.148	13.85

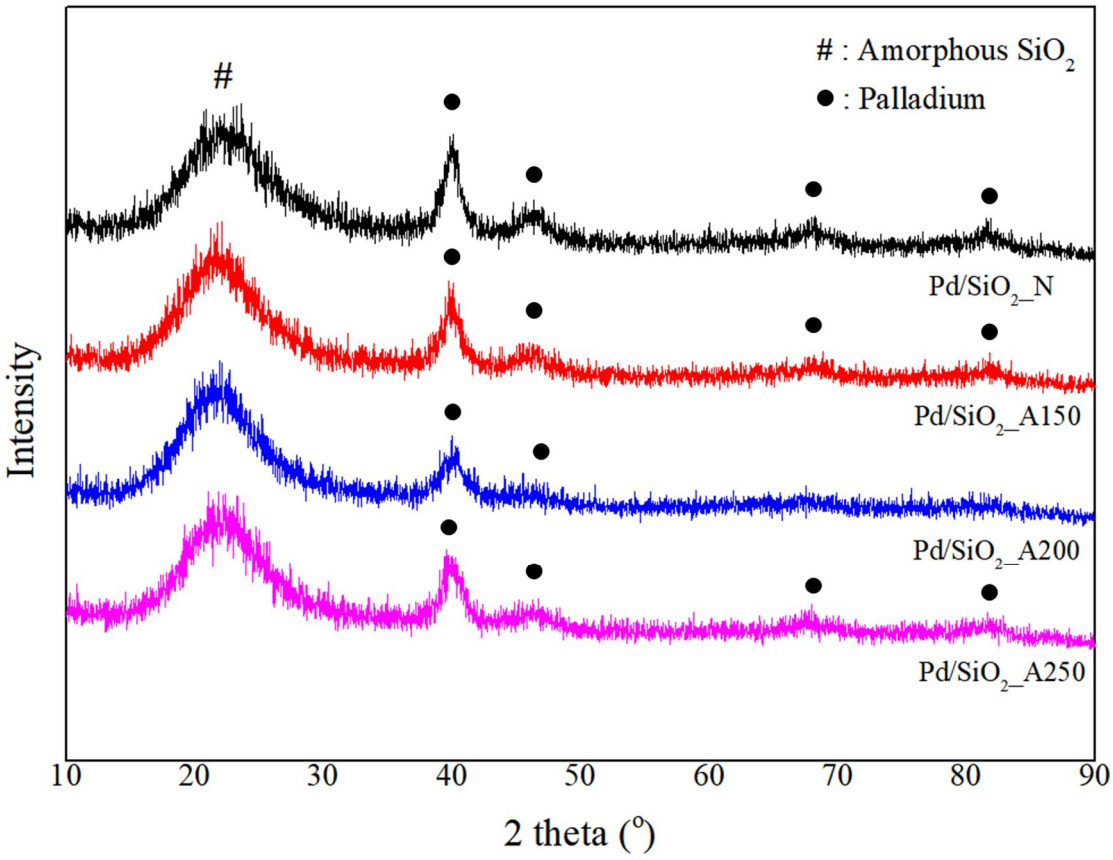

Fig. 3. 10. XRD patterns of Pd/SiO_2 catalysts pretreated by ammonia water.

Table. 3. 6 CO-chemisorption results of Pd/SiO_2 catalysts pretreated by ammonia water

Catalysts	Metal dispersion (%)	Cumulative quantity (mmol/g)	Metallic surface area (m^2/g metal)
Pd/SiO_2_N	2.81	0.0059	12.41
Pd/SiO_2 _A150	3.98	0.0093	17.72
Pd/SiO_2 _A200	8.82	0.0207	39.31
Pd/SiO_2 _A250	4.71	0.0110	20.99

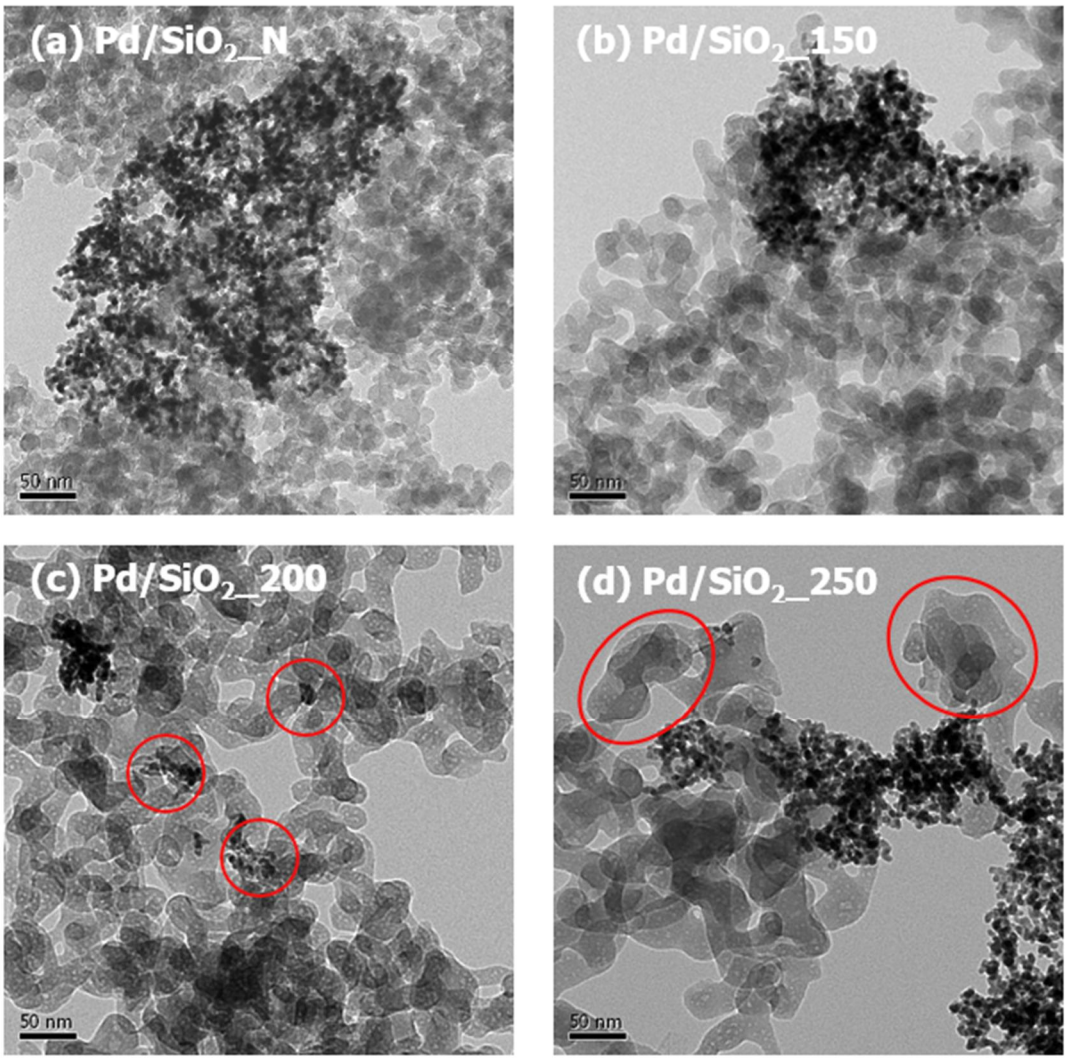

Fig. 3. 11. FE-TEM images of prepared Pd/SiO_2 catalysts by ammonia water.

3.2.3. Dry modification of functional groups by thermal treatment

N_2-phisisorption analysis was performed to investigate the effect of thermal treatment on the pore structure of the support. Table 3. 7 shows the characteristics of the SiO_2 support with different calcination temperature. As indicated, the specific surface area of the support decreased only slightly following an increase in calcination temperature from 300 to 700 °C, while a dramatic reduction was observed at higher temperatures. This is likely due to the aggregation and sintering of the SiO_2 particles above 900 °C [14]. In addition, SiO_2_1100 exhibited a particularly low specific surface area of 0.42 m^2/g, due to phase transition from the amorphous to the cristobalite phase [33].

The XRD profiles of the calcined SiO_2 supports are shown in Fig. 3. 12. As indicated, amorphous SiO_2 was abundant following calcination ≤900 °C. However, following calcination at 1100 °C, peaks corresponding to cristobalite were observed at 2θ = 21.92, 28.38, 31.38, 36.1, 48.52, and 57.06°, due to an increase in the crystallinity of SiO_2 and corresponding phrase transition at high temperatures [33].

In addition to the specific surface area and the phase of silica present, the silanol group concentration on the SiO_2 surface also plays an important role in the dispersion of metal particles on SiO_2 [22, 23]. To examine the influence of calcination temperature on the silanol groups, FT-IR and NH_3-TPD were employed. As shown in the FT-IR spectra (Fig. 3. 13.), Si-O-Si stretching and bending vibrations were observed at 1150, 800, and 480 cm^{-1} in addition to a silanol stretching vibration at 960 cm^{-1} [6, 7]. Upon comparison of the untreated silica support (SiO_2_100), it is clear that high calcination temperatures resulted in decreased quantities of silanol groups, with complete removal being observed at temperatures ≥700 °C [14].

This was also confirmed by NH_3-TPD measurements, as outlined in Table 3. 8, which shows the strength of acidic sites (i.e., silanol groups) on the various calcined supports

[36]. In principle, both the concentration of sites having similar acid strengths and the average adsorption heat or activation energy of NH_3 desorption can be determined using the TPD method. The appearance of the TPD peak was connected with the presence of strongly acidic hydroxyls as sorption sites [37]. As indicated, an increase in the calcination temperature resulted in a decrease in the ammonia adsorption peak areas of the supports, with a sharp drop being observed at temperatures ≥700 °C. Moreover, phase transition at following calcination at 1100 °C resulted in almost complete removal of the silanol groups. The previous studies [5, 7, 25], proved that the surface hydroxyl groups on SiO_2 has a strong interaction with the metal particles, and further affects the metal dispersion and interaction. Based on the different catalytic performances of Pd/SiO_2 catalysts, it is suggested that the change of concentration of silica surface hydroxyls caused by different calcination temperature might be the direct factor for the different catalytic performances.

Table. 3. 7 Textural properties of calcined SiO_2 supports

Supports	Specific surface area (m^2/g)	Pore volume (cm^3/g)	Pore size (nm)
SiO_2_100	172.62	1.122	28.05
SiO_2 _300	150.23	0.663	26.09
SiO_2 _500	132.07	0.699	24.66
SiO_2 _700	119.58	0.517	18.00
SiO_2 _900	51.33	0.190	23.73
SiO_2 _1100	0.42	0.0011	10.96

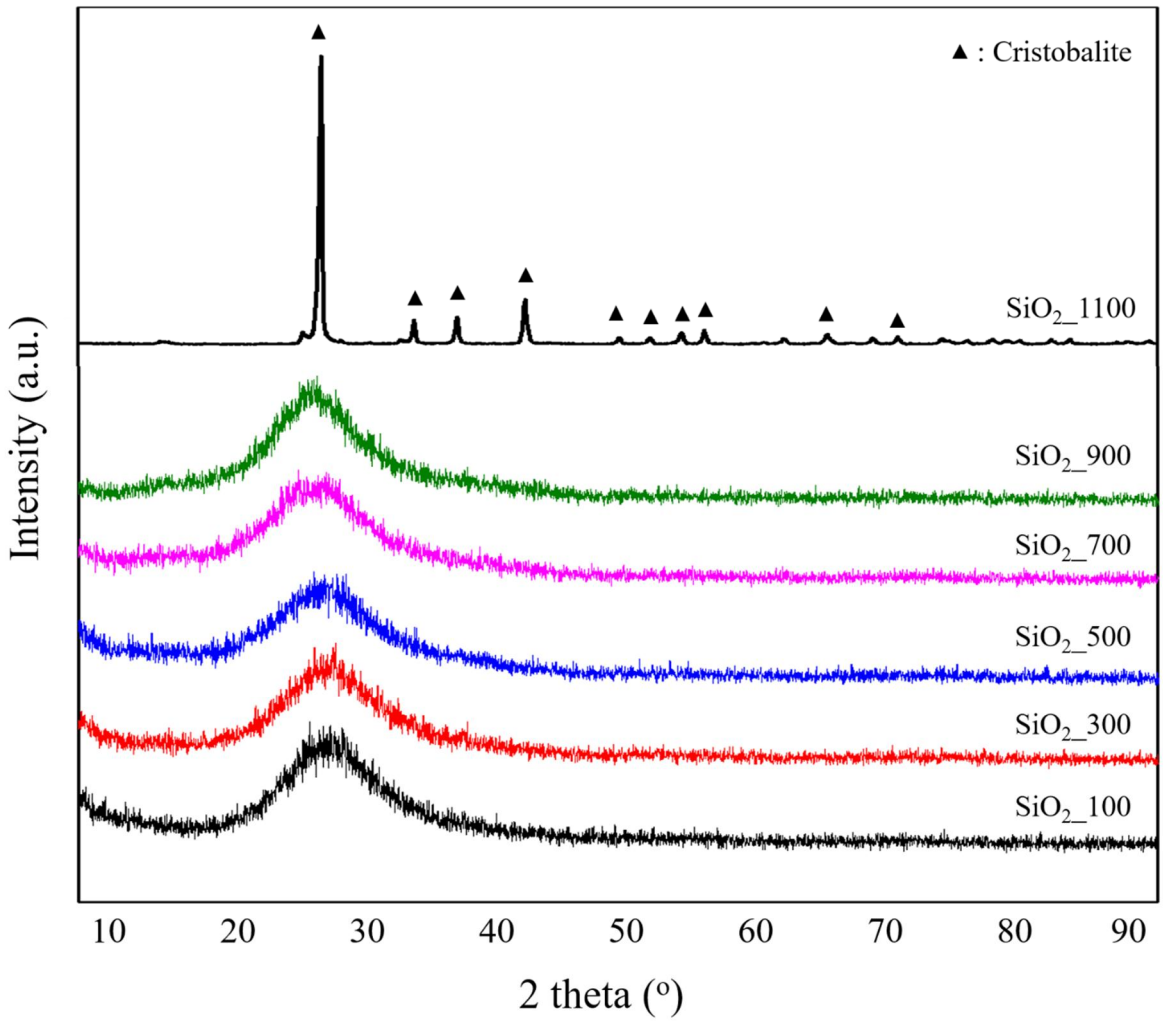

Fig. 3. 12. XRD patterns of calcined SiO_2.

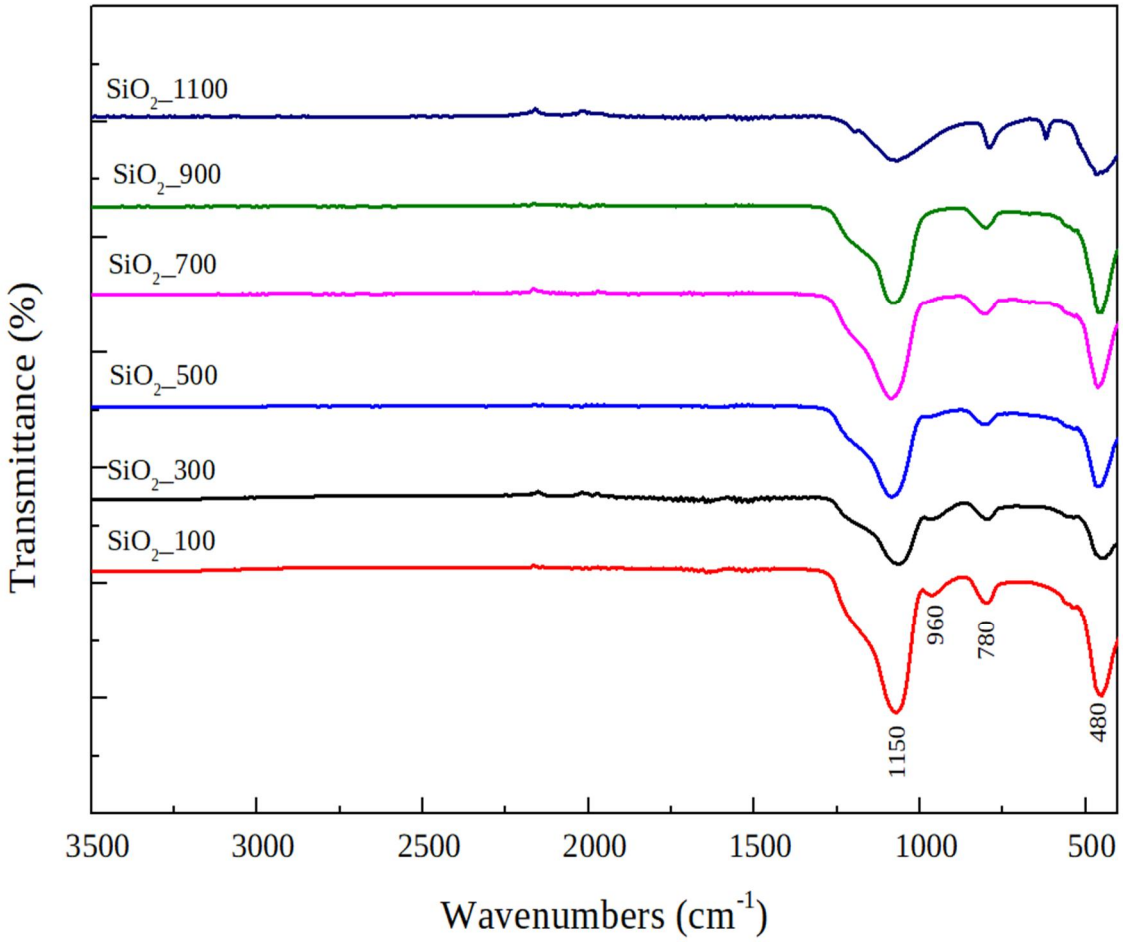

Fig. 3. 13. FT-IR spectra of calcined SiO_2 supports.

Table. 3. 8 NH_3-TPD results of calcined SiO_2 supports

Supports	Acidic site (mmol/g)*
SiO_2_100	1.167
SiO_2 _300	0.728
SiO_2 _500	0.575
SiO_2 _700	0.248
SiO_2 _900	0.271
SiO_2 _1100	0.099

* *Based on NH_3-TPD measurements*

3.2.4. Pd catalysts supported on dry modified SiO_2

The specific surface areas and pore properties of the various catalysts are summarized in Table 3. 9, where slight decreases in the specific surface areas and pore volumes of the Pd-modified catalysts were observed compared with the bare supports [32].

The XRD patterns of the prepared catalysts are presented in Fig. 3. 14., where a broad diffraction peak at 22.21° (corresponding to amorphous silica) is apparent for all supports calcined at temperatures ≤900 °C. In addition, strong diffraction peaks at 40.1, 46.9, 68, and 82.1° were observed for all catalysts, likely due to the presence of crystalline Pd. Those containing calcined supports exhibit significantly broader Pd signals, with Pd/SiO_2_700 having the broadest Pd peak, compared to the Pd peaks for the Pd/SiO_2_100 catalyst. These results suggest that the Pd particles on the SiO_2_700 support are dispersed evenly, as the broad signals are associated with small Pd crystallite sizes [30]. These results correspond closely with the CO-chemisoprtion results.

H_2-TPR experiments were then performed (Fig. 3. 15.) to study the influence of thermal and chemical aging on the reducibility of the Pd species and to understand the role of the silanol groups in the metal-support interactions. As shown in Figure 4, an H_2 uptake peak is present between 50 and 80 °C for all samples [39]. However, upon increasing the calcination temperature to 700 °C, the intensity and area of the signal decreased, and the H_2 uptake peak shifted to lower temperatures. Upon further increasing the calcination temperature above 900 °C, the signal intensity and area increased once again, whilst also shifting to higher temperatures. These results suggest that the Pd species of Pd/SiO_2_700 is the most easily reduced of the various catalysts examined herein [40]. In addition, upon increasing the calcination temperature, strained and weakened siloxane bridges (≡Si-O-Si≡) are formed on the hydroxylated silica surface. At higher temperatures and without vicinal OH groups on the surface, the strained

siloxane groups are converted into stable siloxane bridges and rings. On the basis of our experimental data described above we are of the same opinion which has been stated in a review by Bergna [10] and which can be seen in Fig. 3. 16. Removal of the silanol groups thereby decreases the metal reducibility, while the formation of stable siloxane groups leads to aggregation of the Pd particles. From these results, it is apparent that calcination of the support at 700 °C is the optimal pretreatment temperature for the preparation of highly dispersed Pd/SiO_2 catalysts. Table 3. 10 shows the Pd dispersion percentages as determined by CO-chemisorption measurements and calculation of the CO uptake. As indicated, the metal dispersion increased upon increasing the calcination temperature up to 700 °C, with Pd/SiO_2_700 exhibiting the highest Pd dispersion of 13.02%. The combination of these results with the FT-IR and N_2 physisorption measurements suggests that a decline in the number of silanol groups leads to an increase in metal dispersion, as the silanol groups resulted in strong interactions between Pd and oxygen, thereby inhibiting the reduction of Pd. During the preparation of Pd/SiO_2, the following reactions occurred,

$$\text{surface} \text{–SiOH} \xleftrightarrow{K_1} \text{surface} \text{–SiO}^- + H^+ \tag{3.1}$$

$$\text{surface} \text{–SiO}^- \xleftrightarrow{K_2} \text{surface} \text{–SiOPd}^+ \tag{3.2}$$

$$K_1 = \frac{[\text{surface–SiO}^-][H^+]}{[\text{Surface–SiOH}]} \tag{3.3}$$

$$K_2 = \frac{[\text{surface–SiOPd}^+]}{[Pd^{2+}][\text{Surface–SiO}^-]} \tag{3.4}$$

Van Steen et al [41] suggested that surface-$SiOPd^+$ is the precursor of strong interacting metal species. Substitution Eq. (3.3) into Eq. (3.4) gives:

$$[\text{surface–SiOPd}^+] = K_2[\text{Pd}^{2+}][\text{surface} - \text{SiO}^-] = \frac{K_2K_1[\text{surface–SiOH}][\text{Pd}^{2+}]}{[\text{H}^+]} \quad (3.5)$$

The concentration of surface-$SiOPd^+$ is only proportional to surface of silanol when the Pd salts were fixed. Thus, the higher silanol concentration, the stronger interaction between metal and SiO_2, which will result in low palladium reducibility [12]. that is, removal of the silanol groups enhances metal reducibility [5, 7, 19]. However, the metal dispersions of Pd/SiO_2_900 and Pd/SiO_2_1100 decreased to 7.97 and 5.61%, despite the absence of silanol groups, thereby suggesting dramatic decreases in the specific surface areas and pore volumes of SiO_2 following calcination above 900 °C [9].

Fig. 3. 17. shows the Pd particle sizes and metal dispersions as visualized by FE-TEM. These images confirm an average Pd particle size of ~5–10 nm. In addition, the supported Pd particles become evenly dispersed upon increasing the support calcination temperature up to 700 °C, whilst above 900 °C, condensation of the SiO_2 particles results in sintering. These results support the observations that the removal of silanol groups affects the dispersion of Pd, and that aggregation negatively affects Pd dispersion [9]. It is therefore apparent that the calcination of SiO_2 at an appropriate temperature can improve the dispersion of Pd particles on the support surface.

Table. 3. 9 Textural properties of Pd catalysts pretreated by calcination

Supports	Specific surface area (m^2/g)	Pore volume (cm^3/g)	Pore size (nm)
Pd/SiO_2_100	153.25	0.534	20.67
Pd/SiO_2 _300	148.97	0.576	19.35
Pd/SiO_2 _500	114.36	0.495	21.65
Pd/SiO_2 _700	103.78	0.462	22.421
Pd/SiO_2 _900	50.34	0.133	15.395
Pd/SiO_2 _1100	0.024	0.0015	240.99

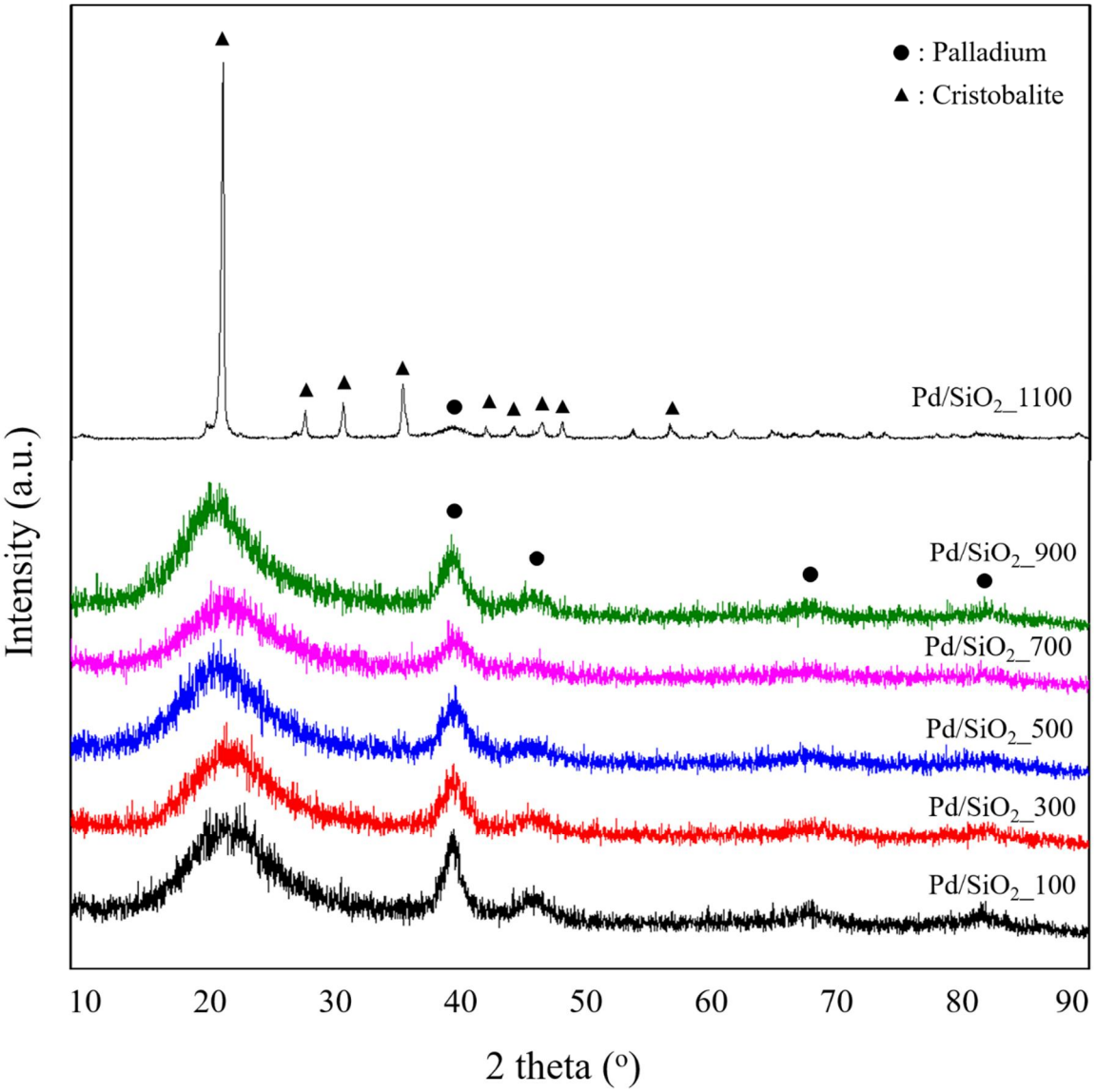

Fig. 3. 14. XRD patterns of Pd/SiO_2 catalysts pretreated by calcination.

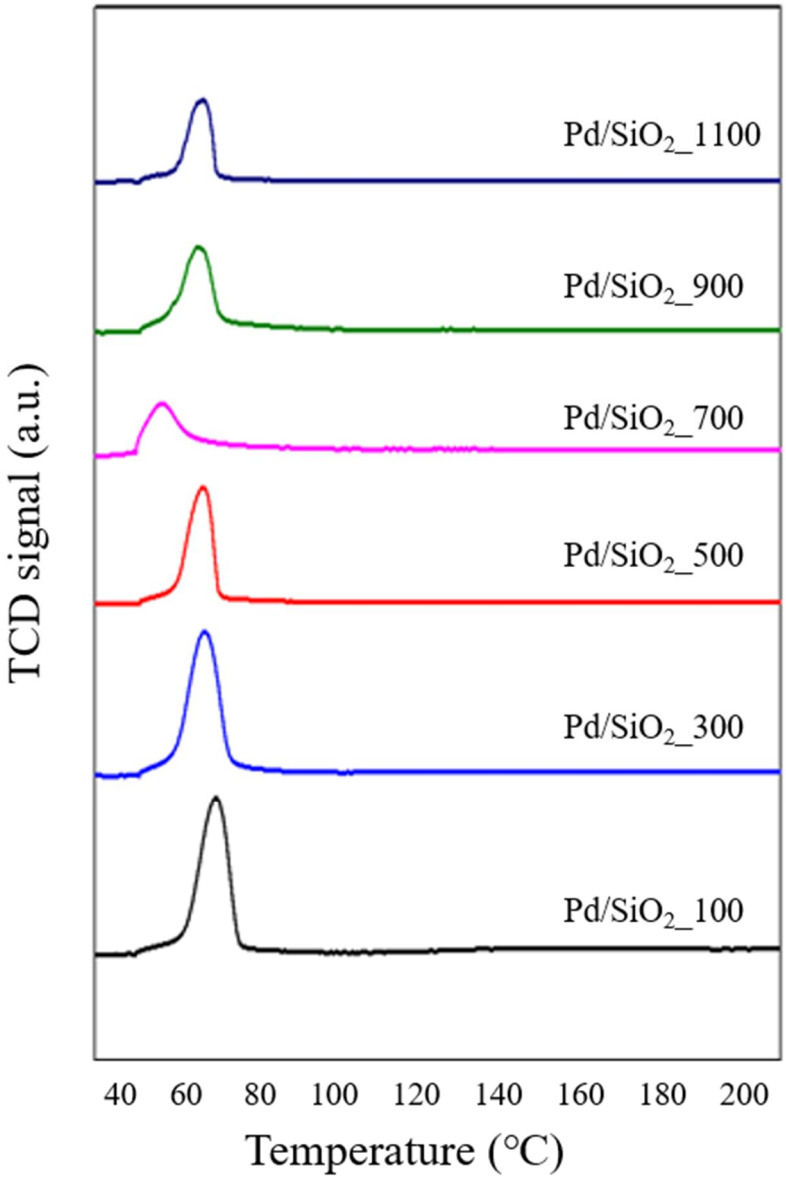

Fig. 3. 15. H_2-TPR profiles of the catalysts pretreated by calcination.

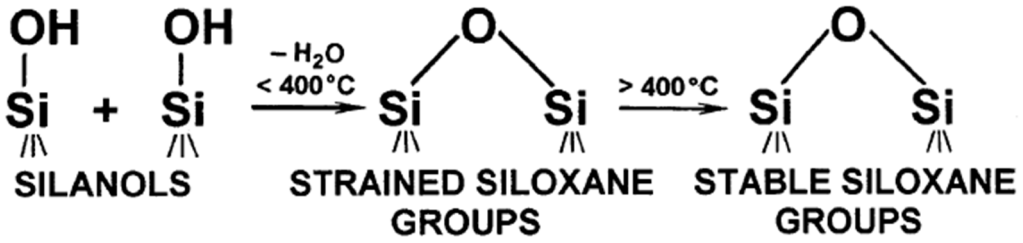

Fig. 3. 16. Modification of silanol groups by thermal treatment (Bergna's scheme) [10].

Table. 3. 10 CO-chemisorption results of Pd/SiO_2 catalysts pretreated by calcination

Catalysts	Metal dispersion (%)	Cumulative quantity (mmol/g)	Metallic surface area (m^2/g metal)
Pd/SiO_2_100	2.90	0.0068	12.93
Pd/SiO_2 _300	5.07	0.0119	22.60
Pd/SiO_2 _500	6.18	0.0145	27.51
Pd/SiO_2 _700	13.02	0.0336	57.99
Pd/SiO_2 _900	7.97	0.0187	35.52
Pd/SiO_2 _1100	5.61	0.0131	24.99

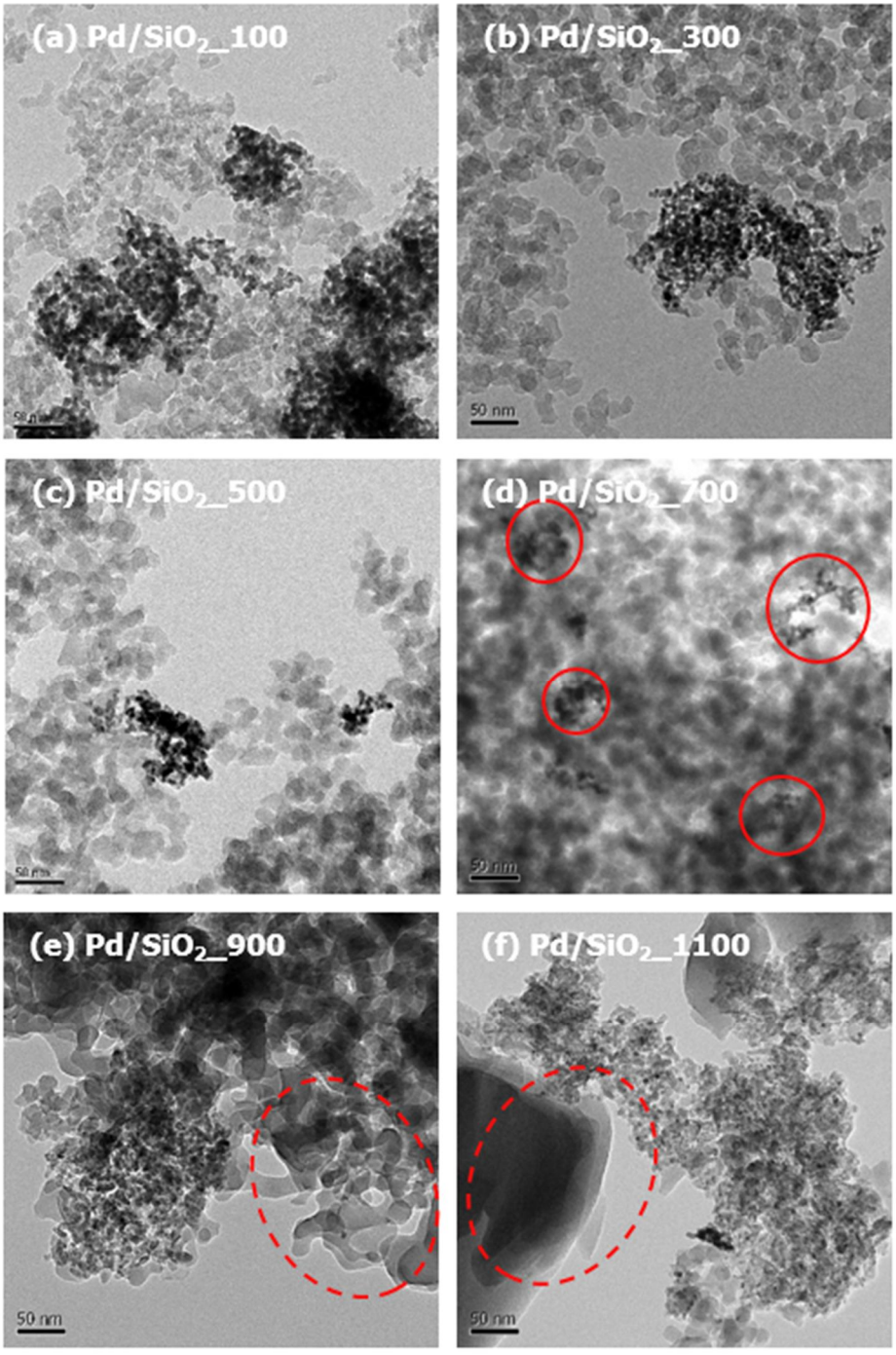

Fig. 3. 17. FE-TEM images of Pd/SiO_2 catalysts pretreated by calcination.

3.3. Catalytic activity on the liquid phase hydrogenation of D-glucose

3.3.1. Effect of reaction time on hydrogenation

To confirm the optimum condition of hydrogenation, catalytic activity test were conducted by varying the reaction time from 4 h to 8 h and maintaining other conditions unchanged (i.e., agitation speed: 1000 rpm; H_2 pressure: 25 bar, reaction temperature: 120 ℃; and catalyst: 5 wt% 0.15 g Pd/SiO_2_700) [42].

Fig. 3. 18. and Table 3. 11. show the conversion of D-glucose, selectivity and yield of sorbitol when the reaction time is varied from 4 to 8 hours in the hydrogenation of d-glucose (the reaction pressure is 25 bar). When the hydrogenation reaction was carried out for 4 hours, the reaction hardly occurred. ($X_{D\text{-}glucose}$ = 16%) and as the reaction time increased, $X_{D\text{-}glucose}$ increased. However, in the hydrogenation reaction at 8 hours, $X_{D\text{-}glucose}$ was increased, but the $Y_{sorbitol}$ decreased because of the yield of fructose, which is a by-product, was increased. Therefore, it was confirmed that when the hydrogenation reaction was carried out for 6 hours, the highest product yield and catalytic activity were obtained.

Table. 3. 11 Effect of reaction time on hydrogenation of D-glucose

Time	Conversion (%)	Selectivity (%)	Yield (%)
4 hr	42.77	79.59	34.04
6 hr	74.35	87.56	65.10
8 hr	87.14	66.71	58.13

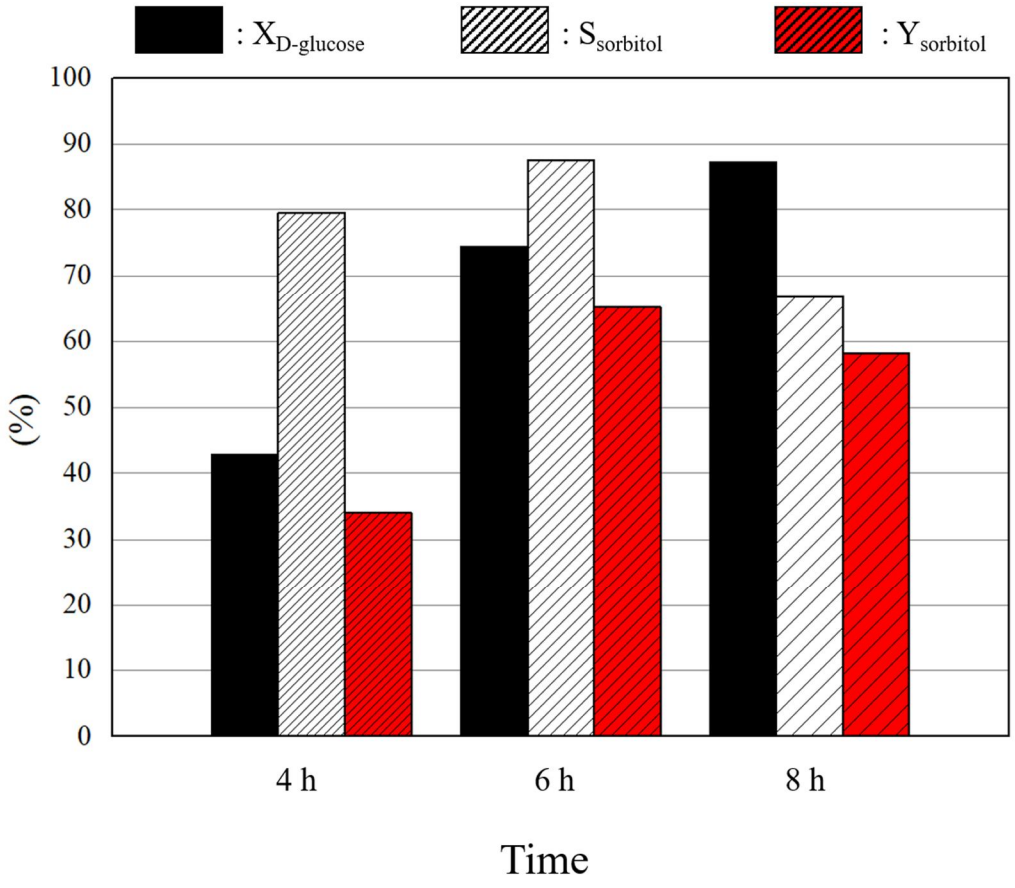

Fig. 3. 18. Diagram of hydrogenation with different reaction time.

3.3.2. Effect of H_2 pressure on hydrogenation

To confirm the effect of the H_2 pressure on hydrogenation, catalytic activity test were conducted by varying the H_2 pressure from 4 h to 8 h and maintaining other conditions unchanged (i.e., agitation speed: 1000 rpm; reaction time: 6 h, reaction temperature: 120 ℃; and catalytic amount: 5 wt% Pd/SiO_2_700, 0.15 g) [42].

Fig. 3. 19. and Table 3.12 show the effect of H_2 pressure on $X_{D\text{-}glucose}$, $S_{sorbitol}$ and $Y_{sorbitol}$ by changing the reaction H_2 pressure to 5-25 bar. From the HPLC results, $X_{D\text{-}glucose}$ and $Y_{sorbitol}$ are increased with increasing the H_2 pressure. When the hydrogenation reaction was carried out under the 5 bar and 15bar, no remarkable differences in $Y_{sorbitol}$ were observed. ($Y_{sorbitol}$ = 6.62 and 26.06%) It is considered that D-glucose was isomerized to sorbitol because of insufficient supply of hydrogen to proceed the hydrogenation reaction. The hydrogen solubility at the gas-liquid interface increase at the high H_2 pressure. The hydrogenation reaction under 25 bar has sufficient supply H_2 to proceed the hydrogenation of D-glucose So it has the highest $S_{sorbitol}$ and $Y_{sorbitol}$.

In the conclusion, It has been confirmed that the highest catalytic activity was observed under the conditions of reaction time, 6 hour and H_2 pressure, 25 bar. And under these conditions, the effect of the metal dispersion of prepared catalysts on the hydrogenation reaction of D-glucose was investigated.

Table. 3. 12 Effect of H_2 pressure on hydrogenation of D-glucose

Pressure	Conversion (%)	Selectivity (%)	Yield (%)
5 bar	15.92	41.61	6.62
15 bar	47.56	54.79	26.06
25bar	74.35	87.56	65.10

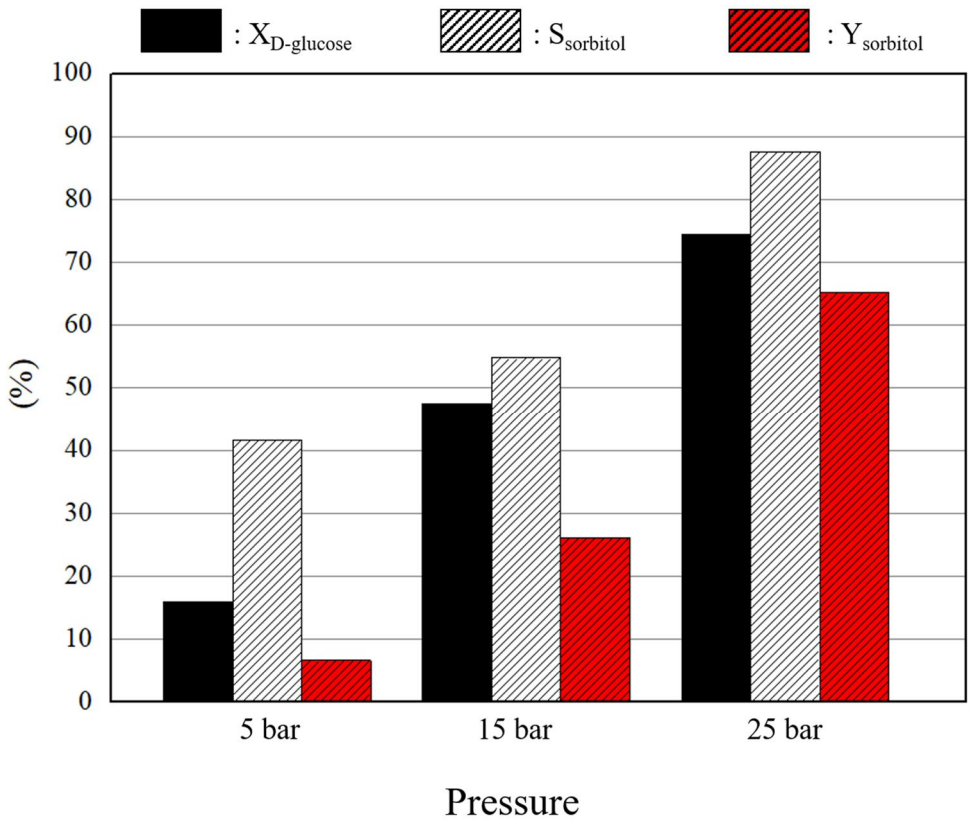

Fig. 3. 19. Diagram of hydrogenation with different H_2 pressure.

3.3.3. Hydrogenation over various catalysts

Hydrogenation was carried out over prepared Pd/SiO_2 catalysts to study catalytic activity depending on the metal dispersion and the properties of supports. The prepared Pd/SiO_2 catalysts were conducted in liquid phase hydrogenation of D-sorbitol under condition (i.e., reaction temperature: 120 ℃; reaction pressure: 25 bar; reaction time: 6 h; and catalytic amounts: 5wt% catalyst 0.15 g) in a 100 mL stainless autoclave.

Fig. 3.20. and Table 3.13. show the catalytic activities of prepared catalysts with OMSs. From the results, the yield of product, sorbitol, is in order to Pd/SBA-15 > Pd/MCM-48 > Pd/HMS as 39.47, 34.11 and 31.26%, respectively. But the activity of the hydrogenation using the three catalysts is almost similar. Because the catalytic activities are related to metal dispersion, all three catalysts with 5-6% Pd dispersion have similar yield of sorbitol.

Fig. 3. 21. and Table. 3. 13. show the catalytic performance of Pd/SiO_2 catalysts pretreated by ammonia water. The yield of sorbitol increased with increase in Pd metal dispersion in the order: Pd/SiO_2_A200 (42.90%) > Pd/SiO_2_A250 (25.25%) > Pd/SiO_2_A150 (15.25%). Among these catalysts, Pd/SiO_2_A200 catalyst exhibited the highest catalytic activity, the sorbitol yield as 42.90%. It is reason that smaller Pd particle and higher Pd dispersion on the SiO_2 exhibited higher sorbitol conversion. The increase of conversion of D-glucose is attributed to this uniform distribution and high dispersion of Pd particles because surface metal Pd atoms is more provided active site with reactant.

The catalytic activities of Pd/SiO_2 catalysts calcined at different temperatures were shown in Fig. 3. 22 and Table 3. 13. The yield of sorbitol increased with increase in Pd metal dispersion in the order: Pd/SiO_2_700 (65.11%) > Pd/SiO_2_900 (44.07%) > Pd/SiO_2_500 (37.34%) > Pd/SiO_2_1100 (35.36%) > Pd/SiO_2_300 (31.73%) > Pd/SiO_2_100 (15.29%). Sorbitol was hardly produced in the absence of a catalyst with

only 2.09% yield. When hydrogenation reaction was carried out using Pd/SiO_2_700 that has the highest metal dispersion, a high yield of 65.10% was obtained. These indicate that the highest yield (using Pd/SiO_2_700) was more than about 4 times the yield of the catalytic reaction with Pd/SiO_2_100.

It is confirmed that the results are related to metal dispersion on hydrogenation of D-glucose since the catalyst with high Pd dispersion collides more efficiently with the reactant compared to the catalyst with low Pd dispersion. These results indicate that the catalyst with high metal dispersion has increased catalytic activity.

Table. 3. 13 Hydrogenation of D-glucose over various Pd/SiO_2 catalysts

Catalysts	Metal dispersion (%)	Activity (%)		
		Conversion	Selectivity	Yield
None	−	19.47	10.72	2.09
Pd/SBA-15	6.18	60.33	65.42	39.47
Pd/MCM-48	5.31	56.52	60.35	34.11
Pd/HMS	5.07	50.94	61.37	31.26
Pd/SiO_2_N	2.81	25.28	60.34	15.25
Pd/SiO_2_A150	3.98	36.62	68.95	25.25
Pd/SiO_2_A200	8.82	60.71	63.36	42.90
Pd/SiO_2_A250	4.71	50.13	67.12	33.65
Pd/SiO_2_100	2.90	25.41	60.14	15.29
Pd/SiO_2 _300	5.07	38.17	83.14	31.73
Pd/SiO_2 _500	6.18	43.92	85.01	37.33
Pd/SiO_2 _700	13.02	74.35	87.56	65.11
Pd/SiO_2 _900	7.97	56.05	78.62	44.07
Pd/SiO_2 _1100	5.61	41.24	85.74	35.36

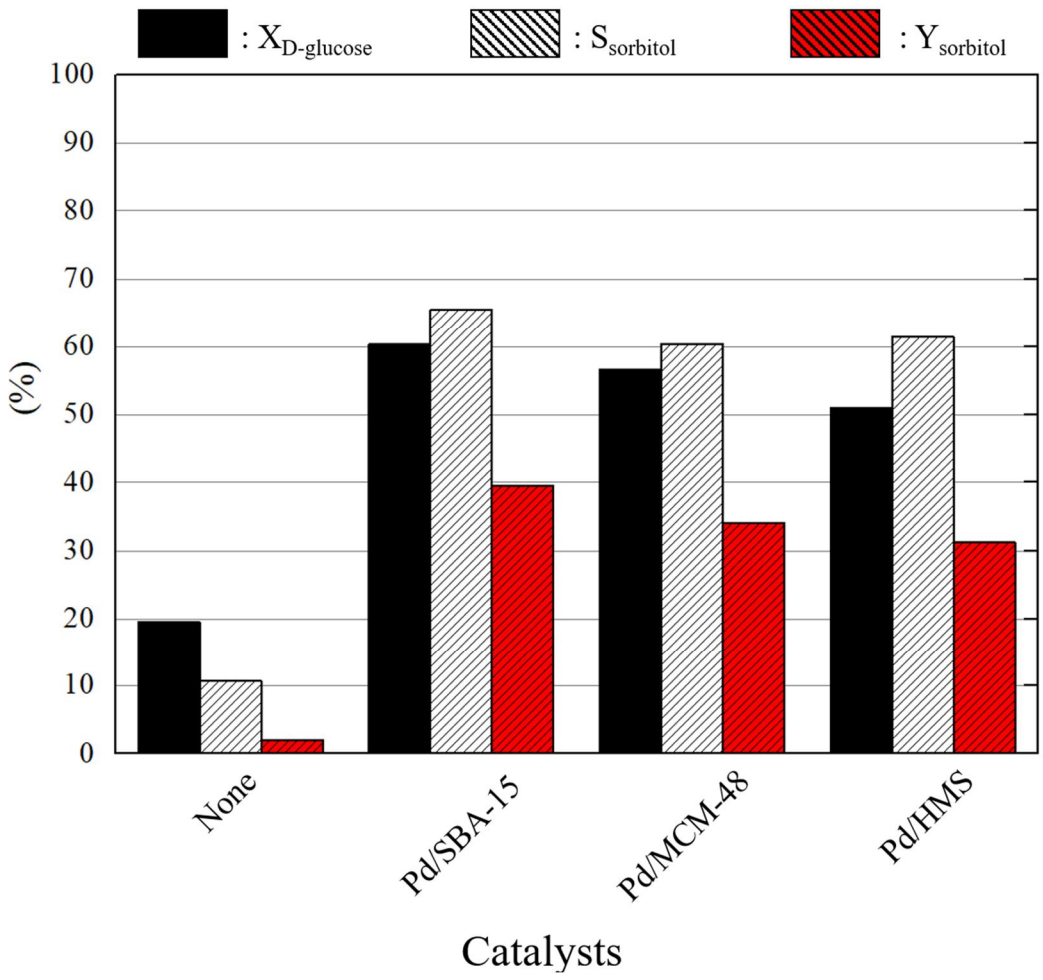

Fig. 3. 20. Diagram of hydrogenation with Pd/OMS catalysts.

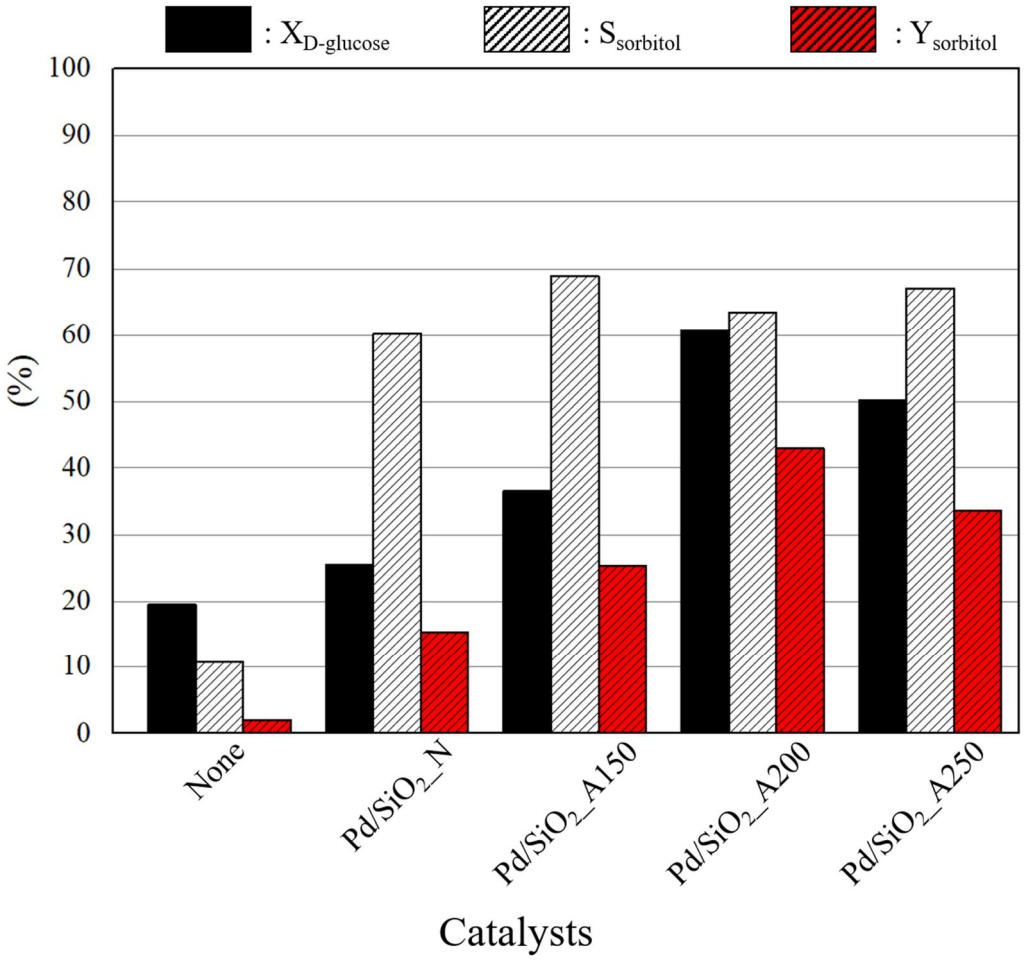

Fig. 3. 21. Diagram of hydrogenation with Pd/SiO_2 catalysts pretreated by ammonia water.

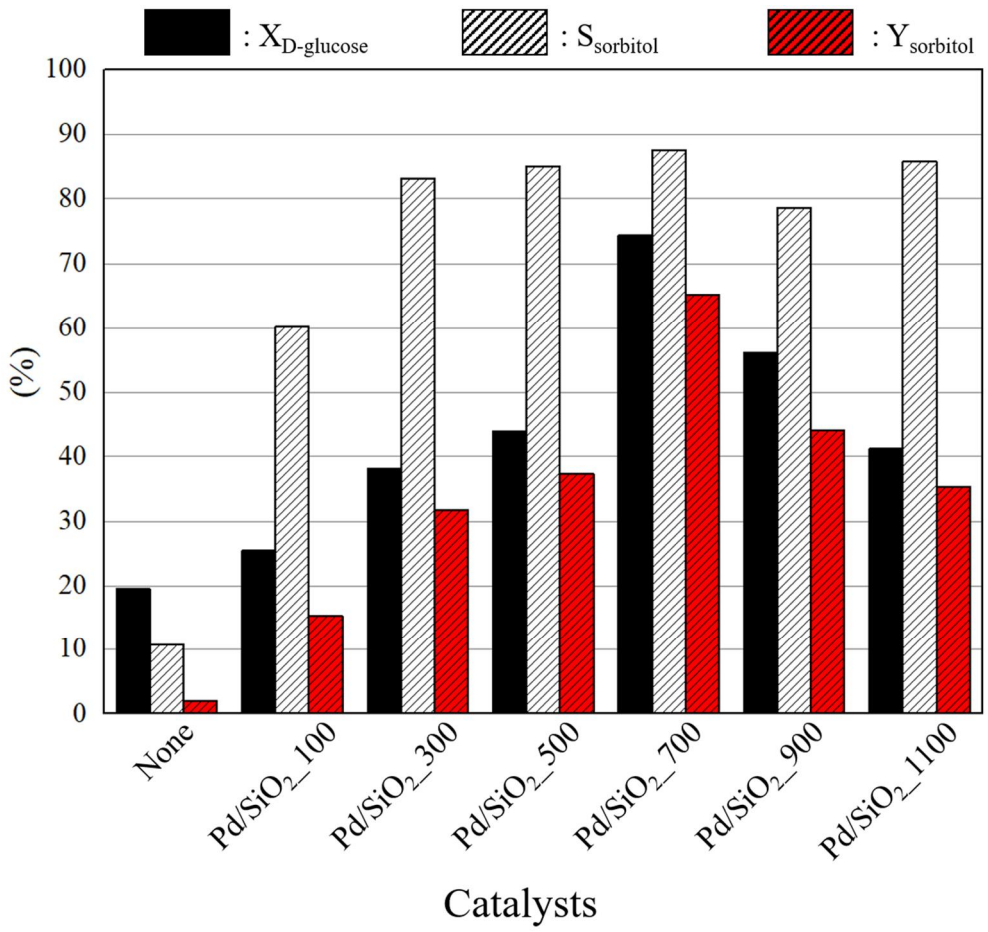

Fig. 3. 22. Diagram of Hydrogenation with Pd/SiO_2 catalysts pretreated by calcination.

3.3.4. Comparison of catalytic activity on the commercial and prepared Pd/SiO_2 catalysts

To compare the catalytic activities of a commercial catalyst (5 wt% Pd/SiO_2 , ThalesNano) and that of a catalyst prepared in this study, liquid-phase hydrogenation of D-glucose was conducted under optimum conditions (25 bar, 120 ℃, 1000 rpm and 6 h). The commercial catalyst was characterization by CO-chemisorption and FE-TEM. Table 3. 16 were listed in the results of CO-chemisorption. The prepared Pd/SiO_2 catalyst has about two times higher metal dispersion of Pd than commercial catalyst. (Pd/SiO_2_700 : 13.02%, Pd/SiO_2_commercial: 7.43%)

Fig. 3. 23. show FE-TEM images of prepared catalyst and commercial catalyst. it can be confirmed that the Pd particles of commercial catalyst are much more tightly aggregated than prepared catalyst.

The catalytic activity results of prepared and commercial catalyst are summarized in Fig. 3. 24. and Table 3. 17. The prepared Pd/SiO_2_700 catalyst has higher yield of sorbitol ($Y_{sorbitol}$ = 65.10%) than the commercial catalyst ($Y_{sorbitol}$ = 38.30%) because of the effect of Pd dispersion and particle size.

Table. 3. 14 CO-chemisorption results of commercial and prepared catalysts

Catalysts	Metal dispersion (%)	Cumulative quantity (mmol/g)	Metallic surface area (m^2/g metal)
Pd/SiO_2_commercial	7.43	0.017	33.09
Pd/SiO_2_700	13.02	0.034	57.99

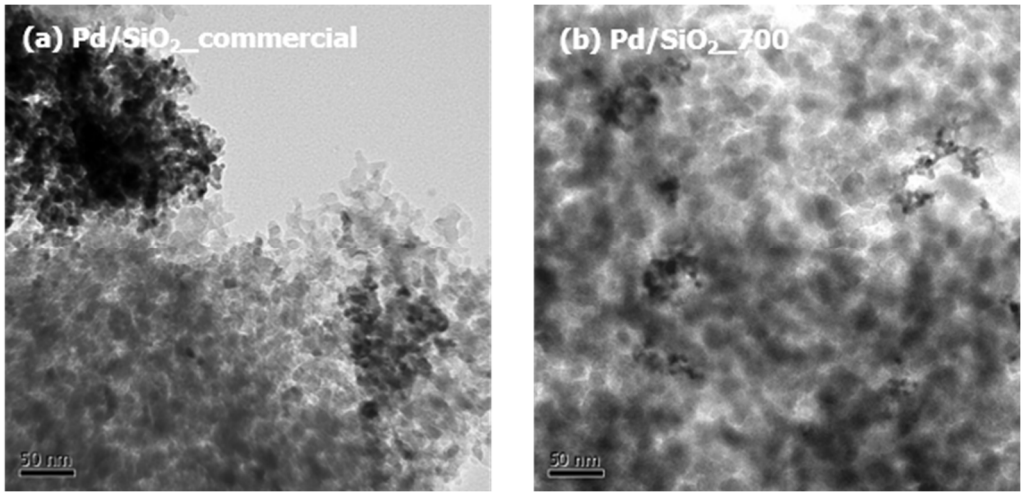

Fig. 3. 23. FE-TEM images of commercial and prepared catalysts;
(a) Pd/SiO_2_commercial and (b) Pd/SiO_2_700.

Table. 3. 15 Comparison of catalytic activity on the Pd/SiO_2 catalysts

Catalysts	D-glucose conversion (%)	Sorbitol selectivity (%)	Sorbitol yield (%)
Pd/SiO_2-commercial	57.54	66.56	38.30
Pd/SiO_2_700	74.35	87.56	65.10

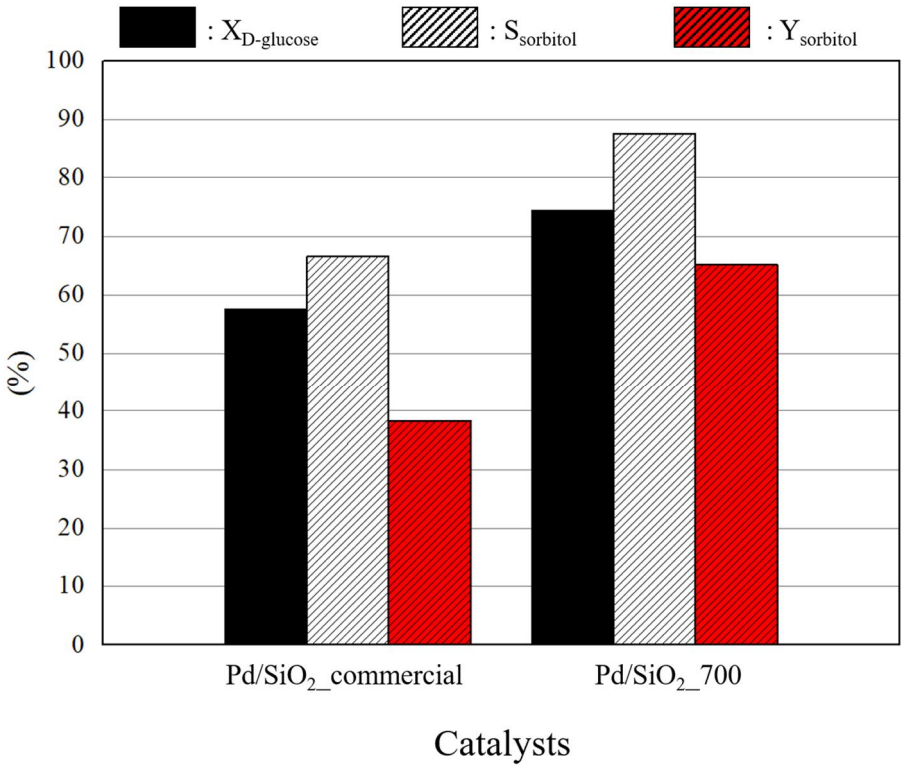

Fig. 3. 24. Diagram of hydrogenation with Pd/SiO_2 catalysts.

4. Conclusion

In this study, the effect of physical and chemical treatment on catalyst preparation was investigated, and also the activity of prepared catalysts was evaluated by hydrogenation of D-glucose. Pretreatment of support is required to produce highly dispersed Pd/SiO_2 catalyst with high activity, because silica has low metal reducibility and low metal-support interaction. And also the hydrogenation of D-glucose was carried out using the prepared catalysts to confirm the effect of metal dispersion on catalytic activity.

1) In order to investigate the effect of physical properties of support on the catalyst preparation, catalysts were prepared using ordered mesoporous silicas (OMSs). Although OMSs having a large specific surface area were expected to be suitable as a support for a high dispersion catalyst, the palladium particles were supported on OMSs with severely aggregated to each other. The catalysts using the OMSs have low Pd dispersion as 5-6%. It is reason that originally silica had low metal-support interaction and OMS has high surface stability caused by the ordered mesoporous structure. These results represent OMS having uniform pore structure is not effective for producing highly dispersed palladium catalyst.

2) To investigate the effect of chemical properties of support on the catalyst preparation, catalysts were prepared using the functionalized silica. Removal of silanol groups lead to increase of the palladium reducibility, because the silanol groups promote strong interactions between Pd and SiO_2. Therefore to prepare the highly dispersed Pd/SiO_2 catalyst, modification of functional groups are necessary. silanol groups can be modified by various treatment such as ammonia water treatment and calcination. From

the result of FT-IR, the silanol groups were completely removed at ammonia treatment temperatures >200 ℃ and calcination temperatures >700 ℃. And the catalysts using these pretreated supports have high Pd dispersion as 8.82% and 13.02%. These results represent the development of a simple method for modification of the surface properties of catalyst supports, which will ultimately lead to enhanced catalytic activities.

3) The Activity of prepared catalysts was evaluated by hydrogenation of D-glucose. From the HPLC results, the hydrogenation using the Pd/SiO_2_700 which has the highest Pd dispersion is has the highest yield of product ($Y_{sorbitol}$ = 65.10%). It is reason that the catalyst having high Pd dispersion has more efficient collision with reactant compared with the catalyst having low Pd dispersion. These results represent that the catalyst which have high metal dispersion has an increased catalyst activity.

5. Reference

[1] J.S. Kim, J.H. Baek, M.H. Kim, S.S. Hong, M.S. Lee, Effect of Carbon Pre-Treatment on Pd Dispersion in Synthesis of Pd/C Catalyst, Mater. Sci. Forum. 804 (2014) 149–152.

[2] F. Patel, Catalyst materials & properties, 2014.

[3] B.K. Min, A.K. Santra, D.W. Goodman, Understanding silica-supported metal catalysts: Pd/silica as a case study, Catal. Today. 85 (2003) 113–124.

[4] S. Alam, S.P. Selatan, P. Pinang, A Review : Mesoporous Santa Barbara Amorphous-15 , Types , Synthesis and Its Applications towards Biorefinery Production, Am. J. Appl. Sci. 7 (2010) 1579–1586.

[5] P.M. Carraro, A.A.G. Blanco, C. Chanquía, K. Sapag, M.I. Oliva, G.A. Eimer, Hydrogen adsorption of nickel-silica materials : Role of the SBA-15 porosity, Microporous Mesoporous Mater. 248 (2017) 62–71.

[6] Z.A. Alothman, A Review: Fundamental Aspects of Silicate Mesoporous Materials, (2012) 2874–2902.

[7] M. Sefara, Pore classification in the characterization of porous materials : A perspective, 5 (2007) 385–395.

[8] K.S.W. SING, D.H. EVERETT, R.A.W. HAUL, L. MOSCOU, R.A. PIEROTTI, Reporting physisorption data for gas / solid systems with Special Reference to the Determination of Surface Area and Porosity, 57 (1985) 603–619.

[9] Z. Qu, W. Huang, S. Zhou, H. Zheng, X. Liu, M. Cheng, X. Bao, Enhancement of the catalytic performance of supported-metal catalysts by pretreatment of the support, J. Catal. 234 (2005) 33–36.

[10] L.T. Zhuravlev, The surface chemistry of amorphous silica. Zhuravlev model, Colloids Surfaces A Physicochem. Eng. Asp. 173 (2000) 1–38.

[11] P.K. Jal, S. Patel, B.K. Mishra, Chemical modification of silica surface by immobilization of functional groups for extractive concentration of metal ions, Talanta. 62 (2004) 1005–1028.

[12] S.H.I. Lihong, L.I. Debao, H.O.U. Bo, S.U.N. Yuhan, Organic Modification of SiO 2 and Its Influence on the Properties of Co-Based Catalysts for Fischer – Tropsch Synthesis, Chinese Jounal of Catalyiss. 28 (2007) 999–1002.

[13] D. Jiang, Y. Ding, Z. Pan, W. Chen, H. Luo, CO hydrogenation to C2-oxygenates over Rh-Mn-Li/SiO2 catalyst: Effects of support pretreatment with nC1-C5 alcohols, Catal. Letters. 121 (2008) 241–246.

[14] R. Lu, D. Mao, J. Yu, Q. Guo, Enhanced activity of CuFe/SiO<inf>2</inf> catalyst for CO hydrogenation to higher alcohols by pretreating the support with ammonia, J. Ind. Eng. Chem. 25 (2015) 338–343.

[15] J.S. Kim, J.H. Baek, Y.B. Ryu, S.-S. Hong, M.S. Lee, Liquid Hydrogenation of Maleic Anhydride with Pd/C Catalyst at Low Pressure and Temperature in Batch Reactor, J. Nanosci. Nanotechnol. 15 (2015) 290–294.

[16] 전학회, 촉매개론, 1989.

[17] K. Van Gorp, E. Boerman, C. V Cavenaghi, P.H. Berben, Catalytic hydrogenation of fine chemicals : sorbitol production, Catal. Today. 52 (1999) 349–361.

[18] T.W. Pacific, N. National, G.P. National, R. Energy, Top Value Added Chemicals from Biomass, 1 (2004) 58–60.

[19] D. Kumar, A. Asharaf, J. Je, S. Hwa, J. Hwang, Selective hydrogenation of d -glucose to d -sorbitol over HY zeolite supported ruthenium nanoparticles catalysts, Catal. Today. 232 (2014) 99–107.

[20] L.M. Sanz-moral, A. Romero, F. Holz, M. Rueda, A. Navarrete, A. Martín, Journal of the Taiwan Institute of Chemical Engineers Tuned Pd / SiO 2 aerogel catalyst prepared by different synthesis techniques, J. Taiwan Inst. Chem. Eng. 65 (2016) 515–521.

[21] D.K. Mishra, J. Lee, J. Chang, J. Hwang, Liquid phase hydrogenation of d -glucose to d -sorbitol over the catalyst (Ru / NiO – TiO 2) of ruthenium on a NiO-modified TiO 2 support, Catal. Today. 185 (2012) 104–108.

[22] P. Gallezot, N. Nicolaus, G. Fl, P. Fuertes, A. Perrard, Glucose Hydrogenation on Ruthenium Catalysts in a Trickle-Bed Reactor, 55 (1998) 51–55.

[23] P.A. Lazaridis, S. Karakoulia, A. Delimitis, S.M. Coman, V.I. Parvulescu, K.S. Triantafyllidis, d -Glucose hydrogenation / hydrogenolysis reactions on noble metal (Ru , Pt)/ activated carbon supported catalysts, Catal. Today. 257 (2015) 281–290.

[24] A. Romero, E. Alonso, A. Nieto-m, Conversion of biomass into sorbitol : Cellulose hydrolysis on MCM-48 and D -Glucose hydrogenation on Ru / MCM-48, Microporous Mesoporous Mater. 224 (2016) 1–8.

[25] D.J. Macquarrie, D.B. Jackson, S. Tailland, K.A. Utting, Organically modified hexagonal mesoporous silicas (HMS)— remarkable effect of preparation solvent on physical and chemical properties, (2001) 1843–1849.

[26] Y. Yang, G. Lv, L. Deng, B. Lu, J. Li, J. Zhang, J. Shi, S. Du, Renewable aromatic production through hydrodeoxygenation of model bio-oil over mesoporous Ni / SBA-15 and Co / SBA-15, Microporous Mesoporous Mater. 250 (2017) 47–54.

[27] G. Lee, Y. Jeong, B. Kim, J. Sae, H. Jeong, H. Bin, J. Chul, Hydrogen production by catalytic decalin dehydrogenation over carbon-supported platinum catalyst : Effect of catalyst preparation method, CATCOM. 67 (2015) 40–44.

[28] A. Romero, A. Nieto-márquez, E. Alonso, Bimetallic Ru : Ni / MCM-48 catalysts for the effective hydrogenation of d -glucose into sorbitol, "Applied Catal. A, Gen. 529 (2017) 49–59.

[29] G. Wang, H. Zhang, Q. Zhu, X. Zhu, X. Li, H. Wang, C. Li, Sn-containing hexagonal mesoporous silica (HMS) for catalytic dehydrogenation of propane : An efficient strategy to enhance stability, J. Catal. 351 (2017) 90–94.

[30] V. V. Dutov, G. V. Mamontov, V.I. Zaikovskii, O. V. Vodyankina, The effect of support pretreatment on activity of Ag/SiO2 catalysts in low-temperature CO oxidation, Catal. Today. 278 (2016) 150–156.

[31] K.J. Folliard, M.D.A. Thomas, B. Fournier, K.E. Kurtis, J.H. Ideker, Interim Recommendations for the Use of Lithium to Mitigate or Prevent Alkali-Silica Reaction (ASR), 2006.

[32] J.S. Kim, S. Hong, J. Kim, M.S. Lee, Effect of Preparation Method for Pd / C Catalysts on Pd Characterization and their Catalytic Activity, Appl. Chem. Eng. 26 (2015) 575–

580.

[33] Y.L. Wei, K.W. Cheng, N. Cheng, H.P. Wang, Effect of silica surface area on molecular structures of lead in thermally treated mixtures of lead acetate and silica oxide, AIP Conf. Proc. 882 (2007) 657–659.

[34] Iler, the chemistry of silica chapter 6: The Surface Chemistry of Silica, Chem. Silica. (1979) 622–729.

[35] C. Brinker, G. Scherer, Sol-Gel Science: The Physics and Chemistry of Sol-Gel Processing, 1990.

[36] S. xian Wang, R. tang Guo, W. guo Pan, Q. lin Chen, P. Sun, M. yuan Li, S. ming Liu, The deactivation of Ce/TiO2 catalyst for NH3-SCR reaction by alkali metals: TPD and DRIFT studies, Catal. Commun. 89 (2017) 143–147.

[37] J.V. Ferenc Lónyi, On the interpretation of the NH3-TPD patterns of H-ZSM-5 and H-mordenite, Microporous Mesoporous Mater. 47 (2001) 293–301.

[38] W. Chen, Y. Ding, D. Jiang, Z. Pan, H. Luo, An effective method of controlling metal particle size on impregnated, 104 (2005) 177–180.

[39] S.K. Matam, E.H. Otal, M.H. Aguirre, A. Winkler, A. Ulrich, D. Rentsch, A. Weidenkaff, D. Ferri, Thermal and chemical aging of model three-way catalyst Pd/Al 2O 3 and its impact on the conversion of CNG vehicle exhaust, Catal. Today. 184 (2012) 237–244.

[40] M.F. Luo, Z.Y. Hou, X.X. Yuan, X.M. Zheng, Characterization Study of CeO2 Supported Pd Catalyst for Low-Temperature Carbon Monoxide Oxidation, Catal. Letters. 50 (1998) 205–209.

[41] E. Van Steen, G.S. Sewell, R.A. Makhothe, C. Micklethwaite, H. Manstein, M. De Lange, C.T.O. Connor, TPR Study on the Preparation of Impregnated Co / SiO 2 Catalysts, 229 (1996) 220–229.

[42] L. Sousa, J. Jose, J.J. De Melo, M. Fernando, R. Pereira, Direct conversion of cellulose to sorbitol over ruthenium catalysts : Influence of the support, Catal. Today. 279 (2017) 244–251.